# Late Paleocene - Early Eocene long and short-term environment and climate change in Southeast Australia

**MSc Thesis**

**Emiel Huurdeman**
**3707210**

**Supervisors:**
**Dr. P.K. Bijl**
**Dr. J. Frieling**
**Dr. F. Peterse**
**Dr. T. H. Donders**
**Dr. A. Sluijs**

**Marine palynology and paleoceanography**

Utrecht University

**Abstract**

The Late Paleocene and Early Eocene are characterized by greenhouse climates, culminating in the early Eocene climate optimum (EECO; 53-50 Ma), the warmest period of the last 65 Myr. Especially the high polar temperature estimates are poorly understood from a climate dynamics perspective; climate modelling studies cannot reproduce the temperatures from proxy data in these areas. In recent years, near tropical temperatures were reconstructed for the Antarctic margin and Tasmania, at a paleolatitude of 60° S, supported by spore and pollen data which suggest vegetation indicative for tropical settings in these areas. This study uses biomarker data ($TEX_{86}$) proxies, dinoflagellate cyst assemblages, and spores and pollen assemblages to reconstruct terrestrial and marginal marine paleoenvironmental conditions during the Late Paleocene and Early Eocene (~57-51.5 Ma) of the Latrobe-1 core on the coast of southeast Australia (paleolatitude ~55° S), with special focus on the Paleocene-Eocene Thermal Maximum (PETM; ~56 Ma). A stratigraphic framework for the sedimentary record was developed using biostratigraphic constraints from dinocysts and terrestrial palynology and bulk organic stable carbon isotope stratigraphy. The $TEX_{86}^{H}$ SST record shows high temperatures (up to 32 °C) in the PETM and EECO, although data suggests an influence of land-derived isoprenoid GDGTs. The abundant tropical pollen and spores and abundance of tropical dinocyst species *Apectodinium* suggest high air and sea surface temperatures during the PETM and towards the EECO. Paleovegetation shows a shift from Late Paleocene rainforest gymnosperm taxa to angiosperm dominated forests towards the EECO, with the introduction of several angiosperm lineages during the PETM and following hyperthermals. These results support the near-tropical temperatures recorded at the Antarctic margin. The paleoceanographic configuration at this location gives an opportunity to assess influence of low latitude surface waters on high latitude climate.

### 1.1 Introduction

Paleoclimatic reconstructions of the Late Paleocene and Early Eocene show the highest global temperatures of the last 65 Myr (Figure 1; Zachos et al., 2008). This greenhouse period is characterized by high atmospheric $pCO_2$-concentrations, estimates from nahcolite proxies range 680–1260 ppmv (Jagniecki et al., 2015), and estimates from $\delta^{11}B$ proxies reach up to 1400 ppmv (Anagnostou et al., 2016), 3-4 times the present day value. Tropical equatorial sea surface temperatures (SST) records show slightly higher SSTs than present (Pearson et al., 2007), while near-tropical sea surface temperature are recorded in polar regions (Sluijs et al., 2008a; Pross et al., 2012), resulting in a low meridional temperature gradient (Bijl et al., 2009; Huber and Caballero, 2011).

Notably, the high polar temperature estimates are poorly understood from a climate dynamics perspective, as climate models have not been able to reproduce the high temperatures obtained from proxy data at high latitudes, both on the short timescale of the Paleocene –Eocene Thermal Maximum (PETM) (Jones al., 2013) and longer timescales of the Early Eocene Climatic Optimum (EECO). Therefore, reconstructing Late Paleocene to Early Eocene paleoclimate is crucial to get a better understanding of Earth's climate system.

The PETM is a hyperthermal event lasting ~150 kyr that occurred superimposed on a warming trend from the Late Paleocene towards the EECO (~53-50 Ma), the warmest sustained temperatures of the Cenozoic. The PETM is associated with a sea surface temperature increase of 5-8 °C based on geochemical Jones et proxies (Jones al., 2013), a negative carbon isotope excursion (CIE) and an abundance of the dinoflagellate genus *Apectodinium* in coastal shelf settings. The 5-8 °C temperature increase in the first <10 kyr of the hyperthermal (Frieling et al., in review) and release of carbon depleted of $^{13}C$ in the ocean and atmosphere in < 5 kyr (Zeebe et al., 2016; Kirtland Turner & Ridgwell, 2016), which indicates a rapid release of carbon of organic source, makes the PETM one of the best paleoclimatic analogues to modern anthropogenic climate change (e.g. Zachos et al., 2008). The high global temperatures of the Late Paleocene and Early Eocene were followed by global cooling that eventually resulted in the Antarctic glaciation in the Late Eocene (Barker et al., 2007) (Figure 1) . This gradual global cooling was interrupted by a short (~500 kyr) warm interval termed the Middle Eocene Climatic Optimum (MECO), at around 40 Ma.

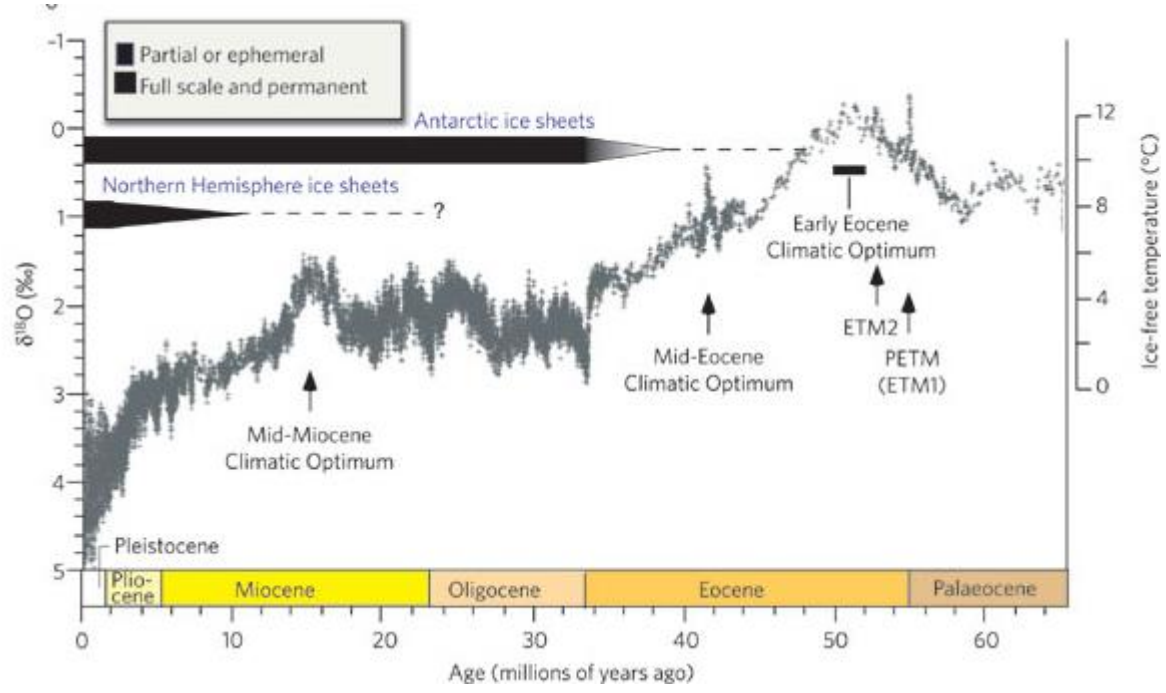


***Figure 1.*** *Oxygen isotope composie of the last 65 Myr. The PETM, ETM2, EECO and MECO are indicated. After Zachos et al. (2008).*

In the Late Paleocene and Early Eocene, the Southwest Pacific Ocean was characterized by near-tropical SSTs (e.g. Bijl et al., 2009) and seems, therefore, a particularly susceptible region for increased atmospheric $CO_2$ concentrations. The Southern Ocean region shows the largest mismatch between climate models and proxy data. Moreover, these warm regions are considered to be close to the locus of deep-water formation during the Paleogene (Thomas et al., 2003), which makes the region particularly important to study: regional changes in oceanography and climate should have been directly transported in the deep-sea oxygen isotopes, and subsequently recorded in benthic foraminiferal oxygen isotopes records (e.g. Bijl et al., 2013b).

In the Early Paleogene, the Tasman Gateway between Australia and Antarctica was not fully developed, and circulation through the gateway was restricted by a series of sills, consisting of the Bass sill, Tasmania and the South Tasman Rise (Figure 2). West of the sills, the surface waters in the Australo-Antarctic Gulf (AAG) were fed by low latitude surface waters of the Indian ocean by the Proto-Leeuwin Current (PLC) in a clockwise circulation pattern. At the Antarctic margin of the AAG at IODP Site U1356 (Figure 2), Early Eocene SST records show high temperatures in the marine realm based on organic proxies (Bijl et al., 2013b), as well as at the coastal terrestrial realm, where pollen and spores show vegetation indicative of a tropical biome (Pross et al., 2012; Contreras et al., 2013). These high temperature estimates are difficult to put into perspective because paleoclimatic data from the northern part of the AAG is lacking.

East of the sills, at the East Tasman Plateau (ETP), sea surface temperature records (Bijl et al., 2009; Sluijs et al., 2011), dinocyst (Bijl et al., 2013a; Bijl et al., 2013b) and pollen (Contreras et al., 2014) assemblages of the Late Paleocene and Early Eocene show paleoclimates that allow tropical

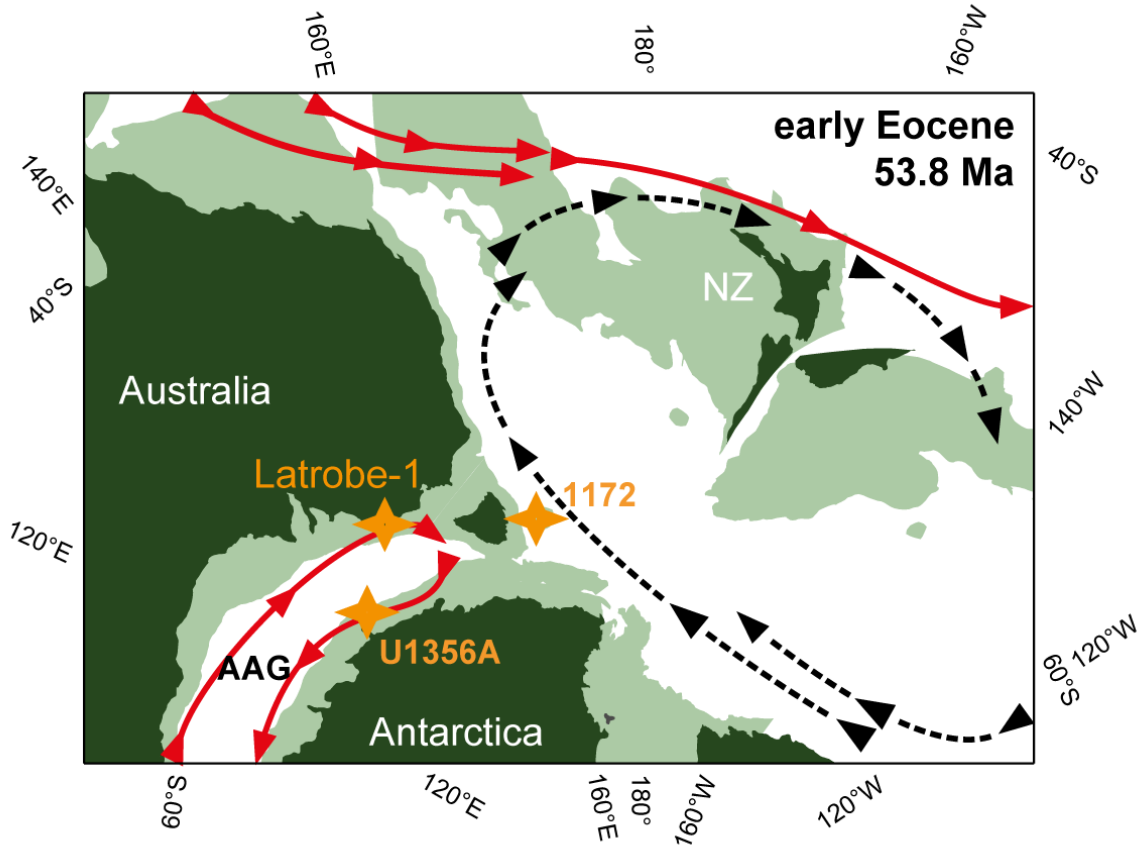


***Figure 2.*** *Configuration of Australia and Antarctica in the Early Eocene. Circulation through the Tasman Gateway is restricted and the Australo-Antarctic Gulf (AAG) is fed by the Proto-Leeuwin Current (PLC). Ocean drilling program (ODP) site 1172 on the East Tasman Plateau and IODP site U1356 on the Antarctic margin of the AAG are indicated. Latrobe-1 is the location of this study. After Bijl & Brinkhuis (2015)*

vegetation for the Early Eocene, while near tropical SSTs are recorded from New Zealand (Hollis et al., 2012). The surface waters east of the Tasman sills were fed by waters from the Antarctic margin by the Tasman Current (Huber et al., 2004). Comparisons of proxy data from the AAG and southwest Pacific ocean are therefore of particular importance to understand the influence of paleoceanographic currents on regional paleoclimate.

Along the southeast Australian margin, the Late Paleocene to Early Eocene is recorded in deposits in the Otway basin, Bass basin, and Gippsland basin (Holdgate & Gallagher, 2003). This study will focus on a paleoenvironmental reconstruction on the Australian margin of the AAG, in the Otway basin (Figure 2 & 3), west of the Tasman sills, to assess the environmental changes of the greenhouse world of the Late Paleocene and Early Eocene in southeast Australia. This study provides the opportunity to put the tropical temperatures that have been reconstructed at the Antarctic margin in a greater perspective. Furthermore, the paleoceanographic configuration at this location gives an opportunity to assess the low latitude influence of surface waters on high latitude climate, especially when results are compared with regions of the Southern Ocean that are influenced by surface waters from high latitude sources, e.g at the East Tasman Plateau.

Here I will investigate the fractional Glycerol Dialkyl Glycerol Tetraether (GDGT) abundances, membrane lipids produced by archaea and bacteria (Schouten et al., 2013). The relative abundances of the different types of isoprenoid GDGTs (*i*GDGTs) show a relationship with SST which can be reconstructed using the $TEX_{86}$ proxy (Schouten et al., 2002). The fractional abundances of branched GDGTs (*br*GDGTs) show a relationship with Mean Air Temperature (MAT), which can be reconstructed using the MBT/CBT proxy (Peterse et al., 2012). As well as biomarker data, dinoflagellate cyst assemblages, and spores and pollen assemblages are obtained to reconstruct terrestrial and marginal marine paleoenvironmental conditions during the Late Paleocene until Early Eocene of southeast Australia. The study will focus on the terrestrial and marine temperature evolution in the north-AAG and biotic responses on environmental change, with special focus on the PETM and the EECO. Dinoflagellate cyst and spores/pollen assemblages will be used as paleoenvironmental indicators as well as dating tool to improve the existing stratigraphic framework. Results will be compared with data from the abundant well-site information in the Otway basin for a regional perspective. Subsequently, the proxy records will be compared to sites outside the Otway basin: e.g., sites on the East Tasman Plateau (ODP site 1172) and the Antarctic margin of the AAG (IODP site U1356) to establish a better understanding of paleoceanography of the Southern Ocean in the Early Paleogene greenhouse world.

### 1.2 Study Site

The Otway Basin is a basin located in southeast Australia that originated as a result of the Late Jurassic – Early Cretaceous rifting between Australia and Antarctic (Yu, 1988; Close et al., 2009). The basin contains a sequence of Mesozoic and Cenozoic sediments that can be up to 13 km thick in the deepest parts of the basin (Megallaa, 1986). The Paleocene- Middle Eocene portion of the sediment sequence, the Wangerrip Group, has been interpreted as coastal plain deposits, characterized by marine sediments with terrigenous input (Holdgate and Gallagher, 2003). Therefore, these sediments give a unique opportunity to connect the paleoenvironmental change of the marine realm with change on the terrestrial realm. The Wangerrip group has been deposited in a system that transitioned from an Early Paleocene transgression to a Late Paleocene/Early Eocene regression (McGowran et al., 2004). The Pebble Point formation overlies the Lower Cretaceous Otway group in outcrop sections, and consist of shallow marine sediments (Holdgate and Gallagher, 2003),

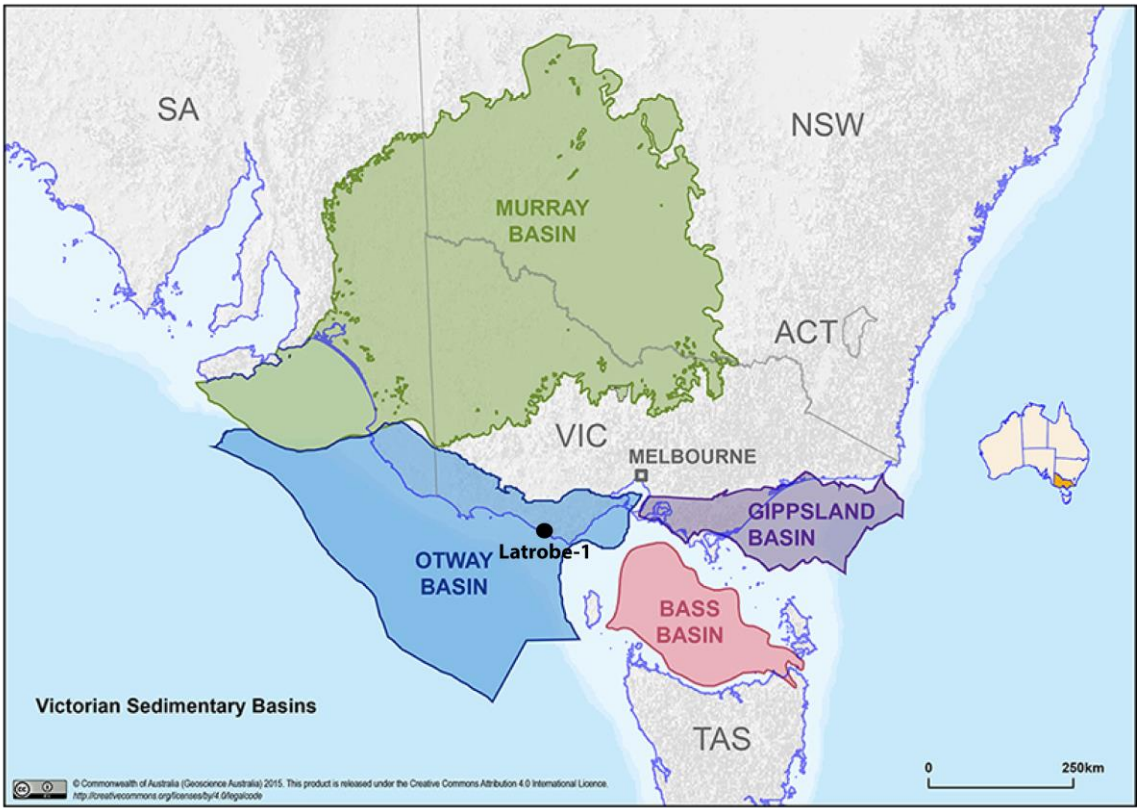


***Figure 3.*** *Location of the Otway basin and adjacent basins shown on southeast Australian margin (Geoscience Australia).The location of Latrob-1 is indicated.*


***Figure 4.*** *Google Earth image of the Eastern part of the Otway Basin. The locations of the Latrobe-1 core and Margaret point are indicated.*

deposited during the initial state of transgression, the overlying pro-delta deposits of the Pember mudstone and the lower delta plain deposits of the Dilwyn formation represent the progradating delta (Edwards et al., 1996).

Within the delta deposits of the Dilwyn Fm., eight smaller order transgression-regression cycles are recognized in the deepest parts of the basin based mainly on well logs and seismics (Arditto,

1995). From outcrop studies of the Wangerrip group, several marine transgressions have been recognized and named by Baker (1950; 1953). These ingressions include the Pebble Point member, the Rivernook-A member, the Rivernook member, the *Turritella* and *Trochocyathus* beds and the Princetown member. The Burrungule member was recognized by Harris (1966) overlying the Princetown member in the Gambier embayment (western Otway Basin), but has thus far not been recognized in the eastern Otway Basin (Holdgate and Gallagher, 2003).

## 2. Materials and methods

### 2.1 Materials

The samples that will be analyzed are recovered from the Latrobe-1 core, drilled near the town of Port Campbell, Victoria, in the eastern part of the Otway basin (Figure 3 & 4) The core is drilled in the southeastern part of the Port Campbell embayment, a lenticular shaped zone that developed during mid-Cretaceous and is shouldered by the Warnambool high in the northwest, the Stoneford high in the east/northeast and the Otway ranges in the southeast (Geological Survey of Victoria, 1995). The core was drilled in 1963 by the Department of Mines of Victoria and spore/pollen (Dettman, 1965; Archer, 1977), foraminifera (Taylor, 1964) and, in recent years, ostracod assemblages (Eglington, 2006; 2014). Taylor (1964) recognized distinct foraminifera fauna from outcrop sections of the Pebble Point, the Rivernook-A, Rivernook member, the *Turritella* bed, *Trochocyathus* bed and the Princetown member in the Latrobe core. This study will use Taylor's (1964) fauna assignments to the Latrobe-1 core and will assess its validity using the obtained stratigraphic data from the Latrobe-1 core and data from the region published since Taylor's (1964) publication. Well logs were obtained during drilling, including spontaneous potential (SP), resistivity logs (SN, LN, LAT) and sonic logging (δt), which reveal the general stratigraphy of different formations (Figure 5) and allow correlations to other wells in the region.

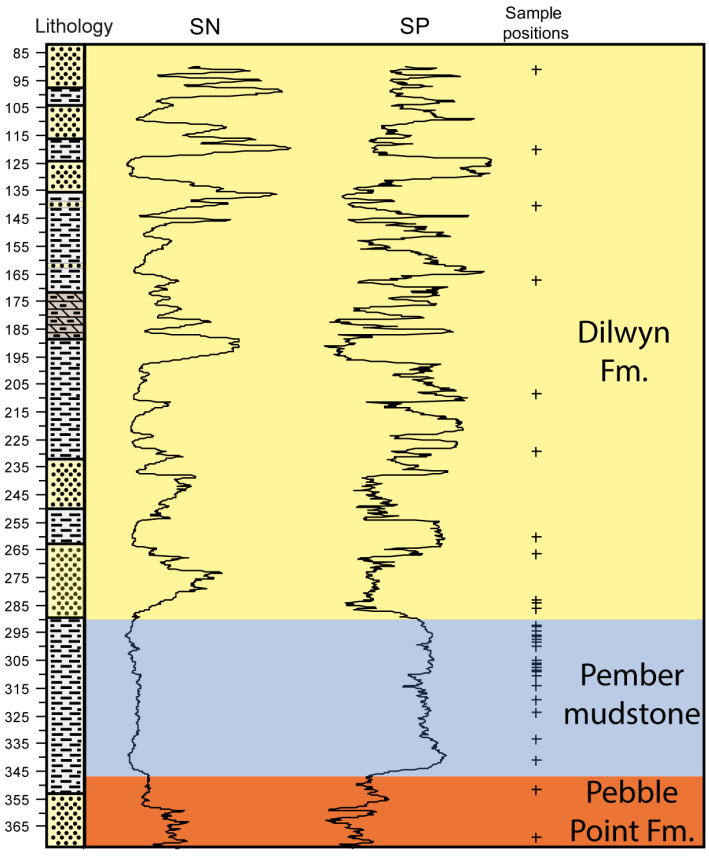


***Figure 5.*** *Well logs showing resistivity log (SN) and spontaneous potential (SP) of the Latrobe-1 core. Sample positions and the formations of the Wanggerip group are indicated.*

While the sequence stratigraphic framework for the Paleocene and Eocene deposits in the Otway basin has been crudely established, little work has been done on the paleoenvironmental conditions that prevailed during deposition in the Otway basin.

Samples were taken from the Latrobe-1 core, obtained from the Werribee core store, Geological survey of Victoria, Australia. The sampled

portion of the core spans from the Late Paleocene to the Early Eocene. The PETM has been recognized in the lower portion of the core by a negative peak in $\delta^{13}C_{org}$ values (Bijl, unpublished data). Samples were taken throughout the whole core, with higher resolution across the PETM.

### 2.2 Methods

#### 2.2.1 Biomarkers

Samples were freeze-dried and subsequently powdered by hand using a mortar and pestle. Total lipids were extracted from the crushed sediment by an accelerate solvent extractor (ASE 350, Dionex) using a mixture of dichloromethane (DCM) and methanol (MeOH) 9:1 (v/v) at 100 °C and $7.6*10^6$ Pa. To quantify GDGT-concentrations, an internal standard ($C_{46}$; Huguet et al., 2006) was added. An activated $Al_2O_3$ column was used to separate into apolar, ketone and polar fractions, using a hexane:DCM 9:1 (v/v) solvent (apolar fraction), a hexane:DCM 1:1 (v/v) solvent (ketone fraction) and a DCM:MeOH 1:1 (v/v) solvent (polar). The polar fractions were dried under a $N_2$ flow and redissolved in 150 µl of hexane:isopropyl alcohol (IPA) 99:1 (v/v) and passed over a 0.45 µm PTFE filter. GDGT analysis was performed by the Agilent 1290 Infinity ultra-high performance liquid chromatography (UHPLC) coupled to an Agilent 6130 single quadrupole mass detector (MS) using two silica Waters Acquity UPLC HEB Hilic (1.7µm, 2.1mm x 150mm) columns at 30°C, preceded by a guard column of the same material. GDGTs were separated isocratically using 82% hexane and 18% hexane:isopropanol 9:1 for 25 min at a flow rate of 0.2ml/min, and then with a linear gradient to 70% hexane and 30% hexane:isopropanol 9:1 for 25 min. The GDGTs were ionized using atmospheric pressure chemical ionization with the following source conditions: gas temperature 200°C, vaporizer temperature 400°C, drying gas ($N_2$) flow 6 L/min, Nebulizer pressure 25 psi., capillary voltage 3500 V, corona current 5.0 µA. The $[M+H]^+$ ions were detected in selected ion monitoring (SIM) mode, and quantified using Chemstation software B.04.02. Chromatograms were analyzed by peak integration.

Before n-alkanes analyses, apolar fractions were desulfurized by adding the sample to activated (using 10 M HCL) copper and stirred for one night. The samples were subsequently passed over a $Na_2SO_4$ column, dissolved in 10 µl of hexane and 1 µl was injected in the gas chromatographer (GC). Gas chromatography was performed using a Hewlett-Packard (HP6890) instrument equipped with an on-column injector and a flame ionization detector (FID). A fused silica capillary column (25 m x 0.32 mm) coated with CP Sil-5 CB (film thickness 0.12 µm) was used with helium as carrier gas. The samples were injected at 70°C and the oven temperature was programmed to 130°C at 20°C/min and then at 4°C/min to 320°C, at which it was held for 20 min.

#### 2.2.2 Proxies

$TEX_{86}^H$ values were calculated for the GDGT-distributions by the calibration of Kim et al. (2010):

$$TEX_{86}^H = \log \frac{(GDGT-1+GDGT-2+Cren')}{(GDGT-1+GDGT-2+GDGT-3+Cren')}$$

Sea surface temperature was calculated using the $TEX_{86}^H$ calibrations:

$$SST = 68.4 \times TEX_{86}^H + 38.6$$

($R^2$= 0.87; n=255; P<0.0001)

The high terrestrial input that is expected because of the coastal proximity of the site could potentially distort the marine $TEX_{86}$ signal, as soil organic matter has been shown to contain *i*GDGT-1, *i*GDGT-2, *i*GDGT-3 and crenarcheol (Schouten et al., 2013). Presence of methanotrophic archaea also have the potential to distort the $TEX_{86}$ signal, especially during methane gas hydrate release, the latter beingGDG proposed as a cause to the PETM and the Early Eocene hyperthermals. Because of these potential distortions the $TEX_{86}$ values of the Latrobe-1 have been evaluated in several different ways, using the BIT-index value, the Methane index MI and the Ring index (RI) and an alternative SST calibration was used alongside $TEX_{86}^H$.

Branched vs. Isoprenoid Tetraether (BIT) index (Hopmans et al., 2004) was calculated using:

$$BIT = \frac{[Ia + IIa + IIa' + IIIa + IIIa']}{[Ia + IIa + IIa' + IIIa + IIIa'] + [Crenarcheol]}$$

The Methane Index (MI) (Zhang et al., 2011) was calculated using:

$$MI = \frac{[GDGT-1] + [GDGT-2] + [GDGT-3]}{[GDGT-1] + [GDGT-2] + [GDGT-3] + [Crenarcheol] + [Cren']}$$

The Ring Index (RI) (Zhang et al., 2016), the weighted average of cyclopentane moieties, is a way of quantifying the deviation of the *i*GDGT-distribution of your sample to the modern calibration, to assess the influence of non-thermal factors on the distribution. This is done by comparing the RI of the modern $TEX_{86}$ value ($RI_{TEX}$) to the RI of your sample ($RI_{sample}$). The calculations were done using the equations of Zhang et al. (2016):

$$RI_{sample} = 0 \times [GDGT-0] + 1 \times [GDGT-1] + 2 \times [GDGT-2] + 3 \times [GDGT-3] + 4 \times [Crenarcheol] + 4 \times [Cren']$$

The bracketed species of GDGTs in this equation represent the percentage of the sum of *i*GDGT-0-3, Crenarcheol and its regioisomer. The $RI_{TEX}$ follows a quadratic equation:

$$RI_{TEX} = -0.77 \times TEX_{86} + 3.32 \times (TEX_{86})^2 + 1.59$$

Samples are presumed outside the modern calibration if the difference ($\Delta RI = RI_{TEX} - RI_{sample}$) lies outside the 95% confidence interval (0.3 units).

An alternative calibration was constructed and successfully applied to samples 4 km southeast of Latrobe-1 at Margaret Point (Frieling, pers. comm.). This calibration was constructed using the global core-top dataset of Kim et al., (2010). Only data points with SST > 10 $^oC$ were used, as the relationship of GDGTs with temperature is shown to be non-linear at low temperatures (e.g. Kim et al., 2010). Removing the low temperatures from the calibration result in higher coefficients, and this has been shown to improve the $TEX_{86}^H$ calibration (Kim et al., 2010). Temperatures below 10 $^oC$ are not expected in the Southeast Australian Late Paleocene and Early Eocene. The ratio between Crenarcheol and its regioisomer (Cren') is used, as this ratio has the lowest potential to be influenced

by high terrestrial input and methanothrophic archeae. The ratio was log-transformed before a linear fit was applied. Hereafter, this calibration will be referred to as the 'Frieling calibration':

$$SST = \log\frac{(Cren')}{(Cren' + Crenarcheol)} \times 16.548 + 43.387$$

($R^2$= 0.69)

### 2.2.3 Palynology

*2.3.3.1 Sample processing*

Samples were freeze dried an subsequently crushed into small chips and weighed. The samples were placed into plastic bottles and a Lycopodium tablet with a known amount of spores was added. Samples were wetted by 10% (v) Agepon wetting detergent and first 10% (v) HCL was added to dissolve the Lycopodium tablet, then 30% (v) HCL, to remove the carbonate. Samples were left to settle overnight, decanted, diluted with water, centrifuged (760 × g for 5 min), and decanted again. Silica was removed by adding 38% (v) HF and placed on a shaker table for two hours, after which the bottles were filled with water and left overnight. Samples were decanted again and 30% (v) HCl was added, centrifuged and decanted. Because of the high amount of silica in the samples, the removal of silica by HF and subsequent washing with HCL was performed twice.

Samples were sieved over a 250 µm sieve, to remove larger particles, and subsequently sieved over a 10 µm sieve. During sieving, an ultrasonic bath was used to disintegrate palynodebris, amorphous organic matter and clay, and to separate heavier particles. The latter was done by placing the sample in a ceramic bowl and let the heavier particles settle down for 5 minutes in the ultrasonic bath. The samples were transferred to test tubes, centrifuged, decanted and diluted with glycerine water. One drop of the sample was transferred to a microscope slides and sealed with nail polish. Two slides were made per sample.

*2.3.3.2 Identification of the sporomorph assemblages*

Slides were analyzed with a light microscope (Olympus CX21). Pollen and spores were counted to an average of 250 specimens and dinocysts, where possible, to 200 specimens. Pollen and spores identification was done using published literature of the region, including Harris (1965), Stover and Partridge (1973), Partridge (1999), Machpail et al. 1994, Macphail (1999), Milne (1988), Pocknall & Crosbie (1982), Contreras et al. (2013), Foster (1982) Cookson (1950) and Raine et al. (2011). Nearest living relatives are from Macphail et al. (1994) and Raine et al. (2011), unless stated otherwise. Dinocysts taxonomy follows the index of Fensome & Williams (2004) and updates from the dinoflaj website. The only exception being the taxonomy of the Wetzeliellioideae, which will not follow the recent proposed change in taxonomy by Williams et al. (2015), but will retain the taxonomy from before their contribution, for reasons that are laid out in Bijl et al. (2016). Dinocyst species encountered that were first described after Fensome & Williams (2004) follow the dinocyst taxonomy of their first described publication (e.g. Sluijs et al., 2009a).

A biostratigraphic framework has been established on the basis of the spore/pollen and dinocyst biozones of Southeast Australia by Partridge (1999; 2006), the dinocyst zonation of the Southern Ocean by Bijl et al., (2013a) and the dinocyst zonation of New-Zealand by Wilson (1988). Partridge (1999) correlated his biozones to planktonic foraminiferal zones, which were later correlated with the GTS 2004 timescale (Partridge, 2006). The Southeast Australian biozones of Partridge (1999; 2006), based on the GTS 2004 timescale (Gradstein et al., 2004), were adjusted to the GTS 2012 timescale (Gradstein et al., 2012).

## 3 Results

### 3.1 Biostratigraphy

Biozones in the following section are mainly from Partridge (1999; 2006), unless stated otherwise. For clarity, herafter spore-pollen zones and dinocyst zones are denoted as 'SP' and 'D' respectively. The lowermost part of the core can be assigned to the *Proteacidites angulatus* (SP) zone based on the occurrence of the eponymous species and the *Senegalinium dilwynense* (D) zone because of the lack of dinocysts from the underlying zones, e.g. *Eisenackia crassitabulata.* The last occurrence of *P. angulatus* (between 369.02 m and 351.83 m), is followed by sediments assigned to the *Propylipollis annularis* (SP) zone, based on the common occurrence of the eponymous species. This zone extends to 308.45 m, up until the first occurences of *Matonisporites gigantis* (SP) and *Apectodinium hyperacanthum*. (D) Although the FO of *M. gigantis*) should precede the FO of *A. hypera*canthum by 100 kyr, they occur in the same sample in the Latrobe-1 core. The real first occurrence of *M. gigantis* does not seem to be recorded and therefore the age of this point is assigned to the FO of *A. hyperacanthum* (~56.2). At 299.67 m, the carbon isotope excursion (CIE) of the PETM is recognized (Bijl, unpublished data), together with the FO of *Spinizonocolpites prominatus*, indicating the base of the *S. prominatus* (SP) subzone in the *Malvacipollis diversus* (SP) zone (56 Ma). Between 292.76 and 286.14 m, the LO of *A.hyperacanthum* is recorded, which coincides in time with the base of the *Apectodinium homomorphum(D)* and *Proteacidites grandis (SP)* zones at 56.2 Ma, although clear indicators of the start of this latter zone have not been found. The base of the overlying *Proteacidites tuberculiformis* (SP) zone (~54.5-53.4 Ma) has been recorded at 229.20 m based on the first occurrence of the eponymous species and the short lived occurrence of *Rhombodinium subtile* between 229.20 m and 208.01 m. The first occurrence of *R. subtile* should roughly coincide with the base of the *P. tuberculiformis* (SP) zone, placing the base of the zone between 260.31 and 229.20 m. The base of the *Myrtaceidites tenuis* (SP) zone is recorded at 167.64 m, based on the FO of M. tenuis and the distinct second occurrence of *Proteacidites pachypolus* (SP). Also, the FO of *Cleistosphaeridium polypetellum* (D) can be found here, which can be correlated to the FO of the species at IODP Site U1356 at Wilkes Land (Bijl et al., 2013a). The base of the *M. tenuis* zone should coincide with the base *Homotryblium tasmaniense* (D) zone, but the FO of *H. tasmaniense* is recorded on a higher stratigraphic level in the Latrobe-1 core, at 96.34 m, the highest studied sample in the core. At this level, the species is found in combination with *Systematophora variabilis* (D), which appears in the middle of the *M. tenuis* zone (~52 Ma). *Santalumicidites cainozoicus* (SP) of the overlying biozone is not encountered, indicating the top sample has an age between ~52-51.7 Ma. *S. cainoizoicus* first appearance is recognized a few meters above this sample at ~85 m during the initial palynological analysis (Archer, 1977). The biostratigraphy indicates sedimentation of ~280 m in 5.7 Myr, implying an average sedimentation rate of 4.9 cm/kyr.

Several discrete samples are available from above 96.34 meters, of which one (at 67.35 m) is palynologically processed. This sample has not been counted, but based on the palynomorphs, this sample can be assigned to the Lower *Nothofagidites asperus* spore/pollen zone and the *Achilleodinium biformoides* dinocyst zone, providing an age of 41.0-38.4 Ma. The ~10 Myr difference in this interval suggests early Middle Eocene hiatus (see section 4.1.1).

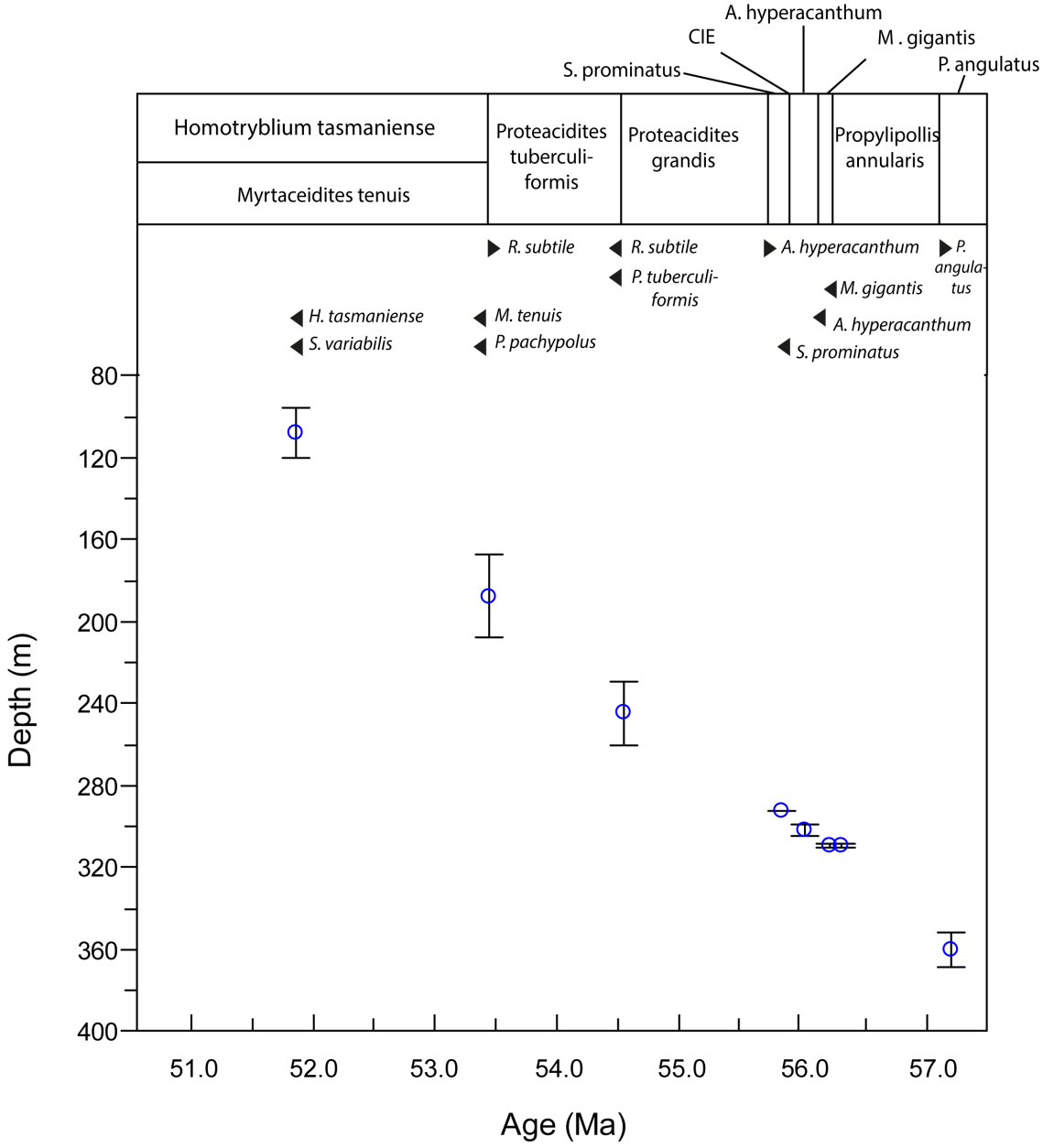


***Figure 6.*** *Age-depth plot based on the sporomorphs of the Latrobe-1 core. Biozones, relevant first and last occurences and chemostratigraphic ie-point (CIE) are indicated.*

### 3.2 Organic biomarkers

The relative abundances of GDGTs of 31 samples were measured, of which 28 samples contained sufficient GDGTs for proxy calculations. The samples show higher concentrations of *i*GDGTs than *br*GDGTs, 0.80 - 21.1 ng $g^{-1}$ for *i*GDGTs and 0 - 8.0 ng $g^{-1}$ for *br*GDGT. SST reconstructions, based on $TEX_{86}^{H}$, show temperatures between 26.9 ˚C and 32.6 ˚C (Figure 9). Although a large amount of scatter is present between samples, a general temperature evolution can be extracted. Late Paleocene temperatures range 27.5-28.5 ˚C, while samples around the PETM, indicated by CIE in the $\delta^{13}C$ values (Bijl, unpublished data), (308-294 m) increase to 28-32.5˚C, with an average of 30.1 ˚C. Early Eocene SSTs range 27.2 ˚C to 32.5 ˚C, with first a decrease in temperature after the PETM at 260-230 m, followed by an increase with peak SSTs at 140 m. While the BIT-index is generally high (average = 0.46), the MAT could not be calculated as the *br*GDGT are almost solely represented by *br*GDGT-Ia.

Frieling calibration SSTs are on average 5 ˚C lower than $TEX_{86}^{H}$ SST, and show a gradual increase in temperature from 22.8 ° C in the Late Paleocene towards 26.7 ° C in the PETM (Figure 9). The record shows a larger cooling in the Earliest Eocene compared with the $TEX_{86}^{H}$ SST record and steady temperatures of 25-26 ˚C from 208.01 meter towards the EECO. The sample at 67.35 m after the middle Eocene (~41-39 Ma) shows SST of 29.3 ˚C and 24.8 ˚C using the $TEX_{86}^{H}$ and the Frieling calibration respectively.

BIT index are generally high (average= 0.46) and show an overall increase in time, from values of 0-0.3 in the Late Paleocene (~370-315 m) to 0.6-0.75 in the Early Eocene (~230-96 m) (Figure 9), with several small dips in BIT index values around the PETM. Methane index (MI) shows relatively low values (0.2-0.3)in the Late Paleocene (~370-315 m), with an increase to values of 0.45 around the PETM (~300-292 m), following a decline to 0.2-0.3 in the Earliest Eocene (~285-260 m) and MI-values > 0.5 in the Early Eocene interval from ~230-96 m.

Only 5 of the 26 samples have a ΔRI < 0.3 (Figure 7A), suggesting influence of the high BIT-index and methanotrophic archaea, as they are both strongly correlated to ΔRI (BIT: $r^2 = 0.62$; MI: $r^2 = 074$) (Figure 7B,C). BIT-index and MI are also correlated ($r^2 = 0.73$) (Figure 7D), suggesting a possible link between these two indices. The possible link between BIT-index has been tested by comparing the *br*GDGT-Ia with the different *i*GDGT concentrations. *Br*GDGT-Ia concentration shows a high correlation with *i*GDGT-1 ($r^2 = 0.68$), *i*GDGT-2 ($r^2 = 0.51$) and *i*GDGT-3 ($r^2 = 0.83$) (Figure 8A), while Crenarcheol ($r^2 = 0.15$ and its regioisomer ($r^2 = 0.06$) show weak to no correlation with *br*GDGT-Ia (Figure 8B).

Gas chromatography (GC) measurements of n-alkanes did not yield results of sufficient quality for further analysis, mainly because of the large abundance of phthalates, a substituent of the plastic bags that were used to store and transport the samples.

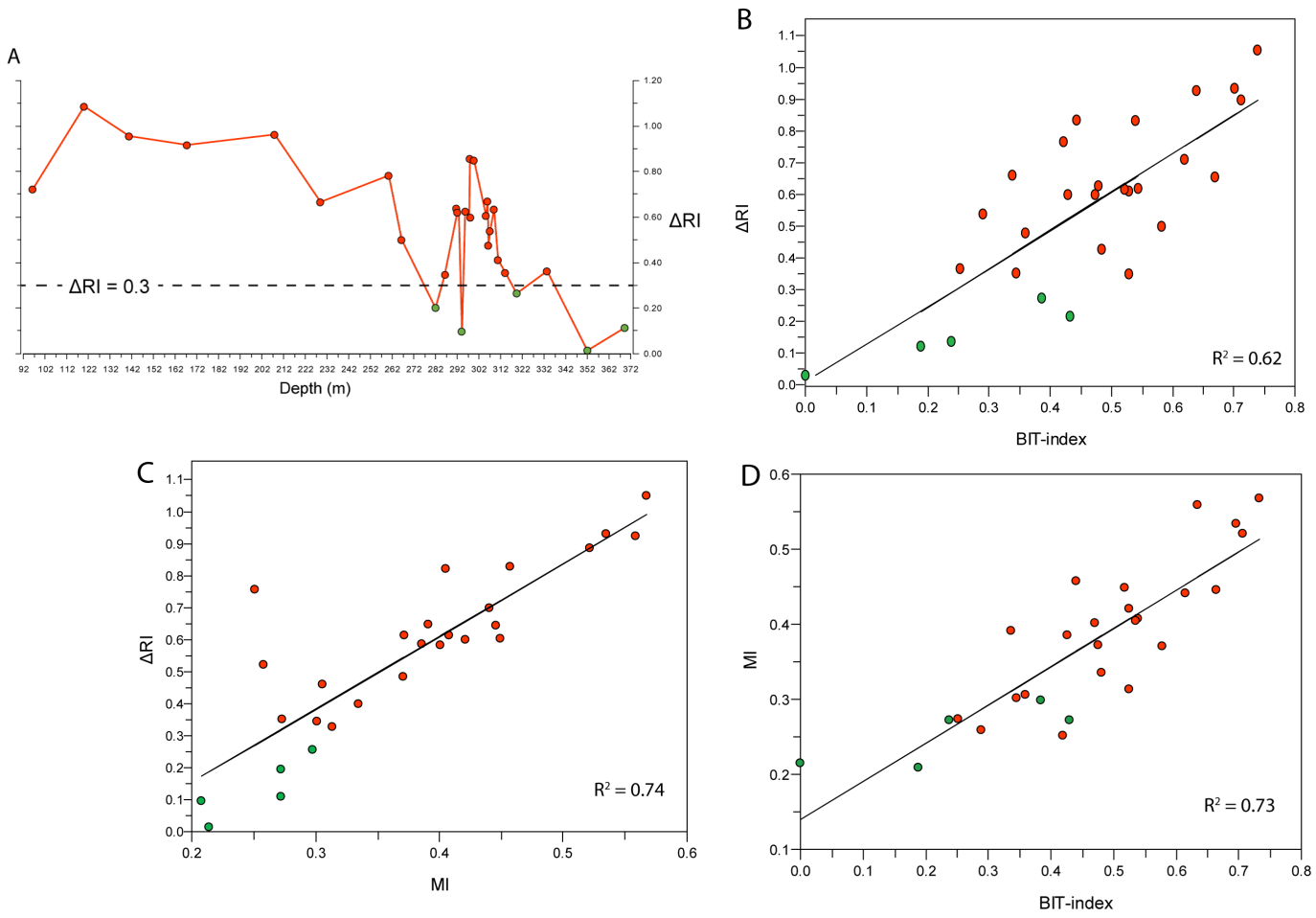


***Figure 7. A)*** *Plot of the ΔRI of the samples. Samples are considered outside the calibration if they fall above the 0.3 line.* ***B)*** *Plot of BIT vs ΔRI with a linear regression line shown* ***C)*** *Plot of MI vs ΔRI with a linear regression line shown.* ***D)*** *Plot of BIT vs MI with a linear regression line shown*

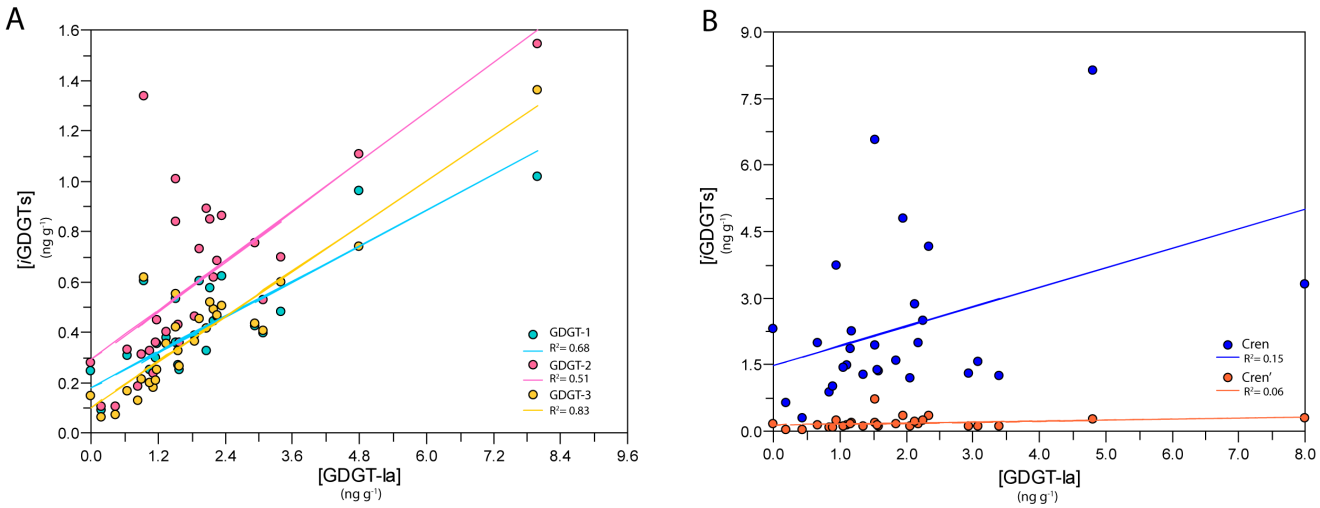


***Figure 8. A)*** *Scatter plot of [GDGT-Ia] and [GDGT-1], [GDGT-2] and [GDGT-3] with the linear regressions of the individual GDGTs shown.* ***B)*** *Scatter plot of [GDGT-Ia] with [Cren] and [Cren'] with their linear regressions.*

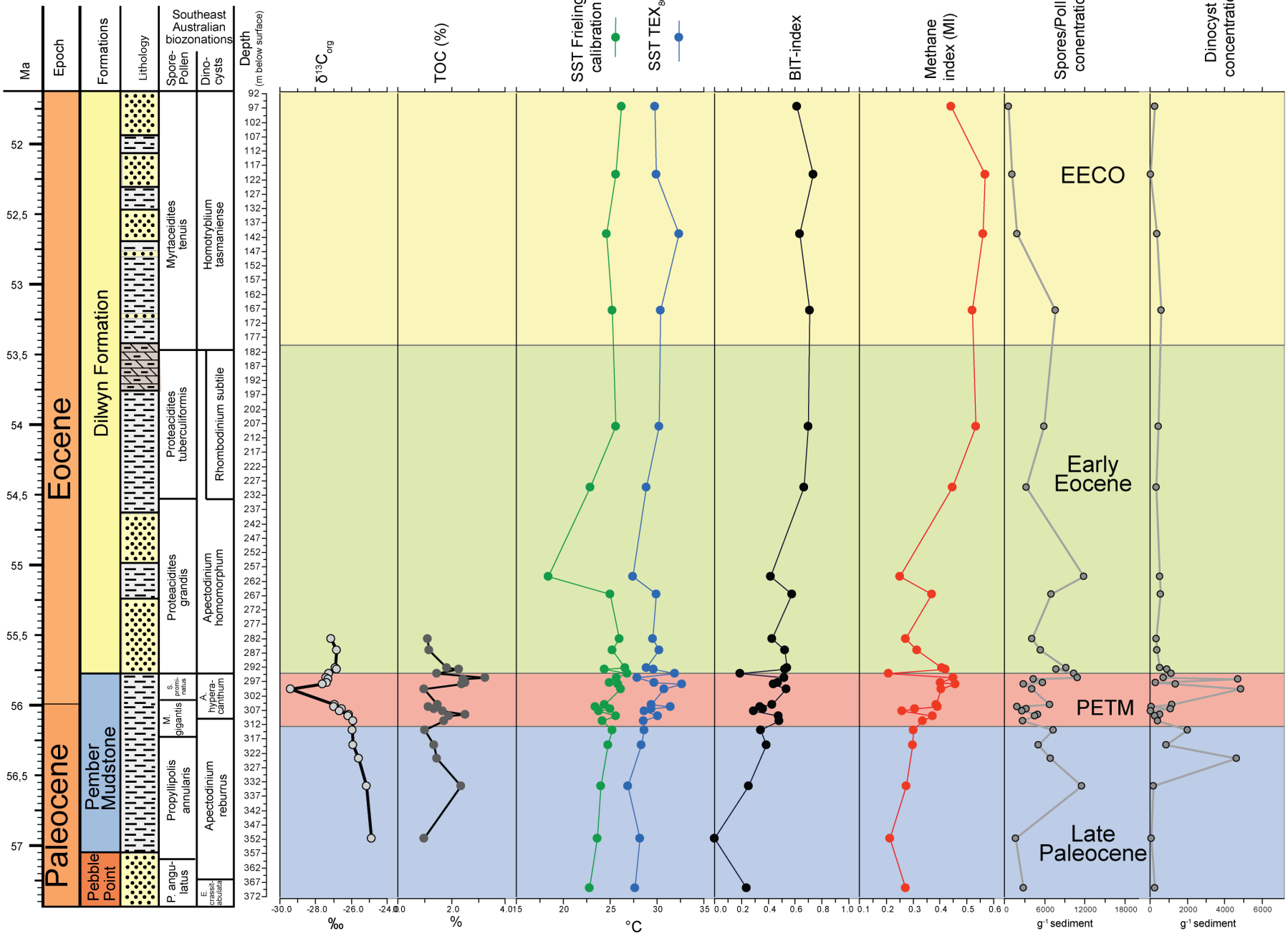


***Figure 9.*** *$TEX_{86}^{H}$ SST, Frieling Calibration SST, BIT index, spore-pollen concentration and dinocyst concentration for the studied interval. $\delta^{13}C$ and TOC (Bijl, unpublished results) are shown to indicate the position of the PETM. Positions of the lithology, biozones and formations are indicated. Color shadings indicate the Late Paleocene, PETM, Early Eocene and EECO.*

### 3.3 Palynology

Palynological assemblages in this marginal marine settings were dominated by terrestrial palynomorphs, (average 79%).Only during the PETM, the dinocyst assemblage reach 50% of the total palynomorphs (Figure 9), mainly due to the high abundance of *Apectodinium*. Acritarchs, commonly in the form of *Paralecaniella indentata* are found in some samples. Plant debris (cuticles and wood particles) and fungal spores are common in most samples.

#### 3.3.1 Dinocyst assemblages

The relative abundances of the dinocyst complexes are shown in Figure 11. The most abundant dinocysts in the Late Paleocene are members of the *Senegalinium* complex, mainly represented by *Phthanoperidinium* and *Senegalinium* species. Other abundant dinocyst are *Deflandrea/Cerodinium* complex, *Glahphyrocysta* complex and *Spiniferites* complex. *Diphyes* spp. *Apectodinium* species become dominant during the PETM, with relative abundances of up to 85%. Just after the PETM (280-290 m), after the LO of A. hyperacanthum at 55.8 Ma, *Spiniferites* complex become abundant, with minor peridinoids represented by *Spinidinium/Vozzhennikova* complex, *Deflandrea/Cerodinium* complex and *Senegalinium* complex. *Apectodinium* reaches a second peak of 60% abundance at 140 m. In the top part of the core, gonyaulacoid dinocysts become abundant, with dominance of *Homotryblium* spp. and *Cleistosphaeridium* spp. Figure 14 shows the dinocyst abundance of the onset and around the PETM (324-280 m). The $\delta^{13}C$ values (Bijl, unpublished data), are shown to indicate the position of the CIE of the PETM. The range chart (See Appendix 4) shows the occurrence of the different dinocysts species over depth, around 60 different species are found throughout the whole core.

#### 3.3.2 Spore and Pollen assemblages

Spore and pollen assemblages in the lower part of the core (370-200 m) are mainly dominated by *Dilwynites* spp. and *Araucariacae* spp., with combined averages of 35%., which decreases In the top part of the core to ~5% (Figure 10). Other abundant species include the bisaccate pollen *Podocarpidites* and spores of the *Laevigatisporites* spp., *Gleichaniidites* spp. and *Cyathides* spp., and the angiosperms *Proteacidites* spp., *Malvacipollis* spp. and *Haloragicidites harissi.* The latter becomes very dominant in the top part of the core, with abundances up to 50%. Minor abundances are found in the saccate pollen *Phyllocladites* spp., *Michroachrydites antarcticus* and the spores of *Peromonolites* and *Clavifera triplex*. Minor angiosperm abundances are represented by Ericipites spp., *Arecipites* spp., *Tricolpites* spp., *Tricolporate* spp. and *Peripollenites* spp.

Gymnosperms are the most common element in the Late Paleocene, accounting for ~65% of the species (Figure 15), while pteridophyte spores are the most abundant component at the onset and during the PETM. Late Paleocene angiosperms are represented by *Proteacea*, *Peripollenites* (?*Caryophyllaceae*)and minor *Casuarinaceae*. Angiosperms have an abundance of 10-30 % in the Late Paleocene and earliest Eocene, only in the late Early Eocene angiosperms become dominant (>50% total abundance). Around the PETM, there is an increase in abundance of *Arecipites* spp. and the first occurrences of *Malvacipollis* spp*., Spinizonocolpites prominatus* (*Nypa* pollen) and *Intratriporopollenites notabilis.* The two latter ones disappears from the assemblages after the PETM, and have a second occurrence in the late Early Eocene.

Diversity of the spore and pollen species, rarefied at 200 specimens, shows an overall increase from the Late Paleocene to the Early Eocene, from an average of 25 species during the Paleocene, to

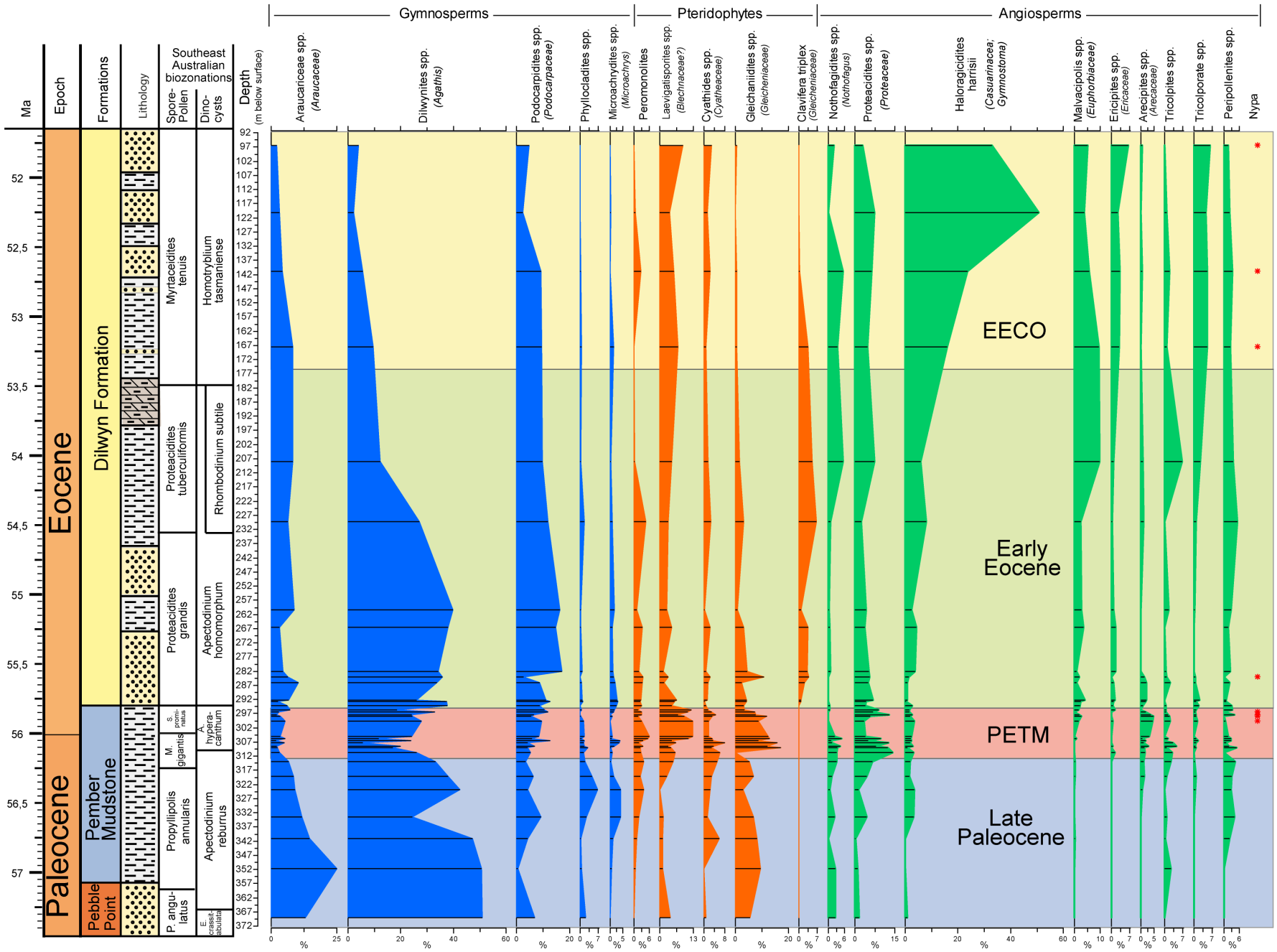


***Figure 10.*** *Spore-pollen assemblages for the studied interval, subdivided in gymnosperms, pteridophytes and angiosperms Positions of the lithology, biozones and formations are indicated. Color shadings indicate the Late Paleocene, PETM, Early Eocene and EECO.*

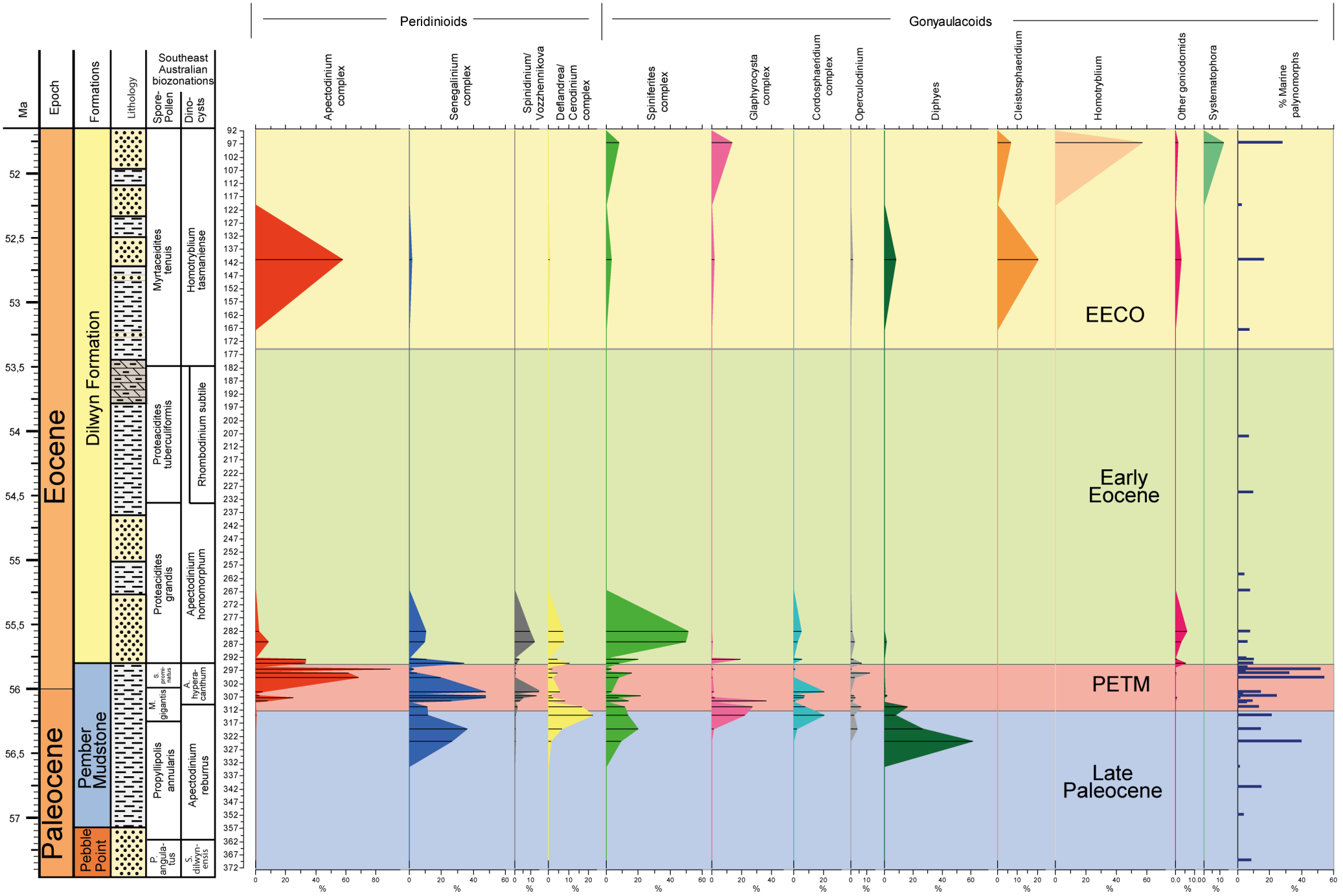


***Figure 11.*** *Dinocyst assemblages for the studied interval and the ratio of marine palynomorphs in the sample. Positions of the lithology, biozones and formations are indicated. Color shadings indicate the Late Paleocene, PETM, Early Eocene and EECO.*

an average of 35 species in the Early Eocene. Exceptions to this overall increase can be found during the decrease towards the lowest $\delta^{13}C$ values in the PETM (~300-308 m) and the at the uppermost part of the core (~90-120 m), where the diversity shows a sudden decrease in number of species (see Appendix 5).

## 4 Discussion

### 4.1 Stratigraphic framework of the Wangerrip group

#### *4.1.1 Latrobe-1 core and outcrop sections*

Results from this work, together with earlier work on the Latrobe-1 core by Taylor (1964) and Eglington (2014), allow for a regional correlation to the outcrop sections of the Paleocene-Eocene stratigraphic record in the Otway Basin. The Pebble Point to the Princetown member have been recognized in the Latrobe-1 core by Taylor (1964), based on foraminifera assemblages. These members are related to eponymous transgressions in the Otway Basin and are possibly correlated to global third order cycles (McGowran et al, 2004). Correlation between these transgressions and sediments in the Latrobe-1 core can therefore act as chronostratigraphic control and aid in uncovering the sea-level history of the AAG.

The Pebble Point formation are shallow marine deposits and part of the initial phase of the transgression which resulted in the pro-delta deposits of the Pember Mudstone. The transition of the Pebble Point formation to the Pember Mudstone in the Latrobe-1 core is placed at ~345 m, based on well logs ( 5) and lithology of the discrete samples, dating the transition at ~57 Ma (Figure 6).

The Rivernook-A and Rivernook Member of Baker (1950), 2 distinct members within the top part of the Pember Mudstone, were placed at ~306-300 m and the ~300-289 m respectively by Taylor (1964). This would mean the Rivernook members comprise the PETM. However, Rivernook (-A) assemblages contain planktonic foraminifera indicative of Early Eocene, after the PETM (Mcgowran, pers. communication). Both Rivernook members in outcrops are sandstone deposits at the top of the Pember mudstone, while the first sandstone deposits in the Latrobe-1 occur in the earliest Eocene (~295 m), just after the PETM. Therefore it seems more likely the Rivernook A member is situated above 295 m in the Latrobe-1 core. This places the Rivernook members in the lower part of the Proteacidites grandis zone (55.8-54.5 Ma).

Based on Taylor's unpublished foraminiferal charts, Eglington (2014) placed the *Turritella* and *Trochocyathus* bands, two thin fossiliferous sandstone beds in outcrops (Stillwell, 2003), at ~262-264 m and ~257 m, respectively. The beds yield a rich fossil assemblage and are considered to indicate a marine transgression (Stillwell, 2003). The two beds are Early Eocene in age, deposited during the *Proteacidites grandis* zone (55.8-54.5) of Partridge (1999, 2006).

The Princetown member of Baker (1953), a carbonaceous sandy shale bed bearing *Cyclammina* foraminifera and outcrops The 'Princetown fauna' was placed at ~229-207 m (Taylor, 1964), based on the distinct fauna. Eglington (2014) noted that the distinctive qualities of the 'Princetown fauna' is not in the uniqueness of the species but rather the proportions of the species and that this interval only yielded low concentrations of forams and intervals with no fauna. The exact location of the Princetown member is therefore hard to infer from the foraminifera data. Spore/pollen data from outcrop sections of the Princetown member (Harris, 1965) can shed some light on this issue. In the outcrop section, the Princetown member contains *Myrtaceidites tenuis* and *Proteacidites pachypolus*

pollen, both indicators for the *Myrtaceidites tenuis* biozone of Partridge (1999, 2006). The FOs of *M. tenuis* and *P. pachypolus* in the Latrobe-1 core are located at 167 m, placing the base of the boundary (~53.4 Ma) somewhere between 208-167 m. Samples in the 229-208 m interval belong to the *Proteacidites tuberculiformis* zone (54.5-53.4), based on the presence of the eponymous species and more importantly, *Rhomboidineum subtile*, which LO is placed at the top of the *P. tuberculiformis* zone. This suggests that the Princetown member is located above 208 m. Moreover, the forams in the outcrop section were assigned to tropical foram zone P7 (McGowran, 2004), which base is halfway into the *M. tenuis* zone (~52.7 Ma) (Partridge, 2006). Dinocysts from the outcrop section of the Princetown member include *Apectodinium homomorphum* and *Diphyes colligerum* (Delfandre & Cookson, 1955), which are both found in the Latrobe-1 at 140.80 meter (see Appendix 3), and both these dinocysts only occur at that position in the upper part of the core. The combination of these biostratigraphic indicators suggest the Princetown member outcrop section correlates with the interval around ~140 meter in the Latrobe-1 core (~52.5 Ma).

The ~10 Myr age difference in the samples between 96.34 m and the 67.35 m Middle Eocene top sample indicate a hiatus, which has been recognized in southeast Australia from the Gulf St. Vincent basin in the west to the Gippsland basin in the east and is commonly referred to as the intra-Lutetian gap, and is at least partially a result of basin inversion, a change to a compressional tectonic regime, starting at ~50 Ma (Holford et al., 2014). The Middle Eocene deposits in the Otway basin comprise of the Nirranda group, and its lowest parts, where the top interval of the Latrobe-1 core presumably belongs to, comprise the Narrawaturk marl (Archer, 1977), a sub-group of the Nirranda group, which outcrops at Ferguson Hill (Tickel et al., 1992).

*4.1.2 Wangerrip group and time equivalents in the Otway and adjacent basins*

The Otway basin forms, together with the Torquay, Bass and Sorell basins, the Northwestern part of the AAG (Figure 3). Late Paleocene-Early Eocene sedimentation in these basins are also named the Wangerrip group, or the equivalent Eastern View group in the Torquay (sub-) basin. The modern Torquay basin is separated from the Eastern Otway by the Otway ranges, although uplift of the ranges had probably not yet been established in the Late Paleocene-Early Eocene (Holdgate et al., 2001). The Eastern View group in Torquay basin is a terrestrial equivalent of the Wangerrip group and is therefore of particular interest as the paleovegetation in the Torquay basin was a possible source area for the terrestrial palynomorphs in the Latrobe-1 core. The Eastern View formation is characterized by several coal seams, deposited in a swamp environment, which correspond to transgressions (Holdgate et al., 2001). The lowermost of the coal seams (coal C) is dated at the base of the Lower *Malvacipollis diversus* (*S. prominatus* and *P. grandis*) zone (~56 Ma) (Holdgate et al., 2001; Holdgate & Clarke, 2000), and is probably laterally equivalent to the upper part of the Pember mudstone. The overlying coal seams B3 and B2 are dated in the Middle *Malvacipollis diversus* (*P. tuberculiformis*) zone, and B3 in the Upper *Malvacipollis diversus* (*M. tenuis and S. cainozoicus*) zone. These coals are harder to correlate to the Latrobe-1 core, because of the lack of resolution and age control at both sites.

The Late Paleocene Wangerrip group deposits in the Bass basin are deposited in a large lake system with a connection to the AAG in the Northwestern part of the basin. In the Latest Paleocene, marine dinocysts are introduced in the lacustrine sediments, which is interpreted as a transgression with a maximum flooding surface (MFS) in the Earliest Eocene (Partridge, 2002), establishing a large lagoon. This transgression can be stratigraphically correlated to the PETM upper part of the Pember mudstone in the Otway Basin, based on palynology. Similarly to the Torquay basin, the Early Eocene

transgressions in this basin in the Middle *Malvacipollis diversus* zone and Upper *Malvacipollis diversus* zone are hard to correlate, because of the age control. However, in the Bass basin the transgressions are accompanied by dinocyst occurrences, two Early Eocene transgressions accompanied by *Apectodinium homomorphum* and the top transgression by *Homotryblium tasmaniense*. It is likely the top transgression is correlated to the *H. tasmaniense* interval in the Latrobe-1 core at 96.34 m and the second *A. homomorphum* transgression in the Bass basin with the second *A. homomorphum* interval at 140.80 m in the Latrobe-1 core.

The Sorell basin has not been extensively studied as the other basins, but the Wangerrip group can be found in the Cape Sorell-1 core (Boreham et al., 2002), and parts of it can be correlated to the PETM upper part of the Pember mudstone in the Otway Basin, and possibly with the *Homotryblium tasmaniense* interval in the Latrobe-1 core at 96.34 m, based on palynology.

### 4.2 Stratigraphy of the CIE and PETM

The $\delta^{13}C_{org}$ record of the Latrobe-1 core records the CIE of the PETM, shown by a ~3 ‰ decrease at the interval between 295-300 m. Only a small section of sediment was recovered from 295-300 m, of which the exact depth is unknown, creating difficulties in identifying the start and assessing the shape of the CIE. Clues about the shape of the CIE can be inferred from the $\delta^{13}C_{org}$ record at Margaret Point (Frieling, unpublished results), an outcrop section ~4 km southwest of the Latrobe core. This outcrop section holds a continuous $\delta^{13}C$ record of the onset of the CIE which can be chemostratigraphically correlated to the Latrobe-1 core, as well as biostratigraphically, the *Diphyes* bloom and the (first) *Apectodinium* acme being the most relevant tie points (Figure 12). Both records, although more pronounced at Margaret Point, show a two-step pattern in the decrease of $\delta^{13}C$ values an initial decrease (position 1 in Figure 12), of ~0.5~1 ‰ that persist ~3-5 m and is accompanied by an *Apectodinium* acme, after which the $\delta^{13}C$ suddenly decreases to ~-30 ‰ (position 2). This initial step is unusual in PETM carbon isotope records, as the large majority show a single decrease in $\delta^{13}C$ values. Signs of a small carbon isotope excursion below the actual CIE are found in carbonate soil nodule $\delta^{13}C$ records from the Bighorn Basin (Wyoming, USA) (Bowen et al., 2015) and marginal marine setting on the New Jersey shelf (Self-Trail et al, 2010), but, as for the southeast Australian records, it remains unclear if this is a local signal. One possible explanation is variability in sedimentation between the 'step' and the 'ramp', the initial step in

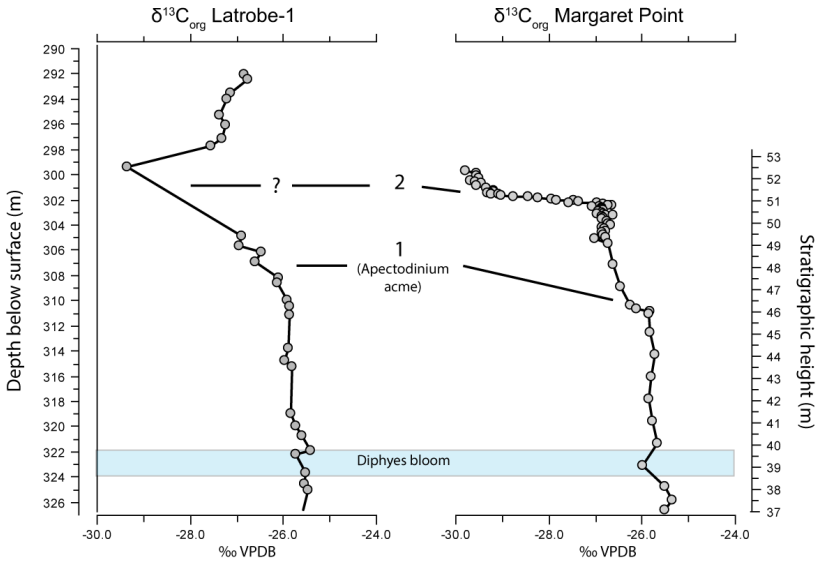


***Figure 12.*** *$\delta^{13}C$ of the Latrobe-1 core (Bijl, unpublished results) and Margaret Point (Frieling, unpublished results). Two positions are proposed for the start of the CIE in both records, (1) the initial decrease(~0.5-1 ‰)in $\delta^{13}C$ values, and (2), the ~3 ‰ decrease towards the lowest values in the records.*

$\delta^{13}C$ at Margaret point is found in a condensed section, a concretionary band often formed during or slightly after sediment starvation. If these sediments are followed by a relatively expanded section this would result in a $\delta^{13}C$ 'ramp' (Frieling, pers. communication). For the Latrobe-1 core, the onset of the CIE, which coincides with the Paleocene-Eocene boundary, is placed at the first decrease in $\delta^{13}C$ values, after position 1 in Figure 12, because the chemostratigraphy of Margaret point seem to suggest that the CIE onset is relatively expanded in the area.

The *Apectodinium* acme precedes the CIE by a few kyrs in several records around the globe (Sluijs et al., 2007b), including ODP Site 1172 at the ETP (Sluijs et al., 2011). The relative timing of the *Apectodinium* acme in these records is hard to constrain, because of the lack of high resolution biostratigraphic data. The *Apectodinium* acme is recorded between the FO of *A. hyperacanthum* at ~309 m and the FO of *Spinizonocolpites prominatus* at ~300 m, which would place the *Apectodinium* acme somewhere in the ~100 kyr interval before the Paleocene/Eocene boundary (Partridge (1999,2006). The presence of the tropical dinocyst *Apectodinium* and change in vegetation (see section 4.4.2.1) implies that climate change preceded the CIE, in agreement with evidence from the ETP (Sluijs et al., 2011), New Jersey, and the North Sea (Sluijs et al., 2007b).

### 4.3 Paleoenvironmental reconstruction

#### 4.3.1 GDGT-distributions and the SST record

$TEX_{86}^{H}$ SST records show tropical temperatures for the northern AAG during the Late Paleocene and Early Eocene. These SST records are accompanied by relatively high BIT-index values and high MI, indicating high terrestrial soil input into the marine realm and influence of methanotrophic archaea respectively (Weijers et al., 2006; Zhang et al., 2016). These influences are quantified by the Ring index (RI) and shows that only 5 samples are within the standard deviation of the RI-$TEX_{86}$ relationship of the global core top dataset (Kim et al., 2010). The RI index is correlated with both BIT and MI, showing that both these factors influence the *i*GDGT concentrations. The RI and BIT are also correlated, although they reflect two different kind of mechanisms, soil input (BIT) versus methanotrophic archaea in the water column (MI). Furthermore, the *br*GDGT-Ia correlates strongly with *i*GDGT-1, *i*GDGT-2 and *i*GDGT-3, suggesting that part of the found *i*GDGTs have a terrestrial origin. The source of these GDGTs could possibly be the methanogenic archaea *Euryarchaeota* which is found in wetlands and peat bogs and are known to produce *i*GDGT-1-3 (Weijers et al., 2006). GDGT contents of modern South African acidic peat bogs near iSimangaliso Wetland Park, show similar relative abundances of GDGTs to the ones found in Latrobe-1, including presence of *i*GDGTs and *br*GDGTs solely represented by *br*GDGT-Ia (Miller, unpublished results). Moreover, the consistent presence of the peat moss *Sphagnum* (*Cingutrilet*es), although only in small amounts (0-3% of the spore/pollen assemblage), suggests that peats were present near the coast. The contribution of terrestrial *i*GDGTs implies the calculated $TEX_{86}$ in the Latrobe-1 is not solely derived from Thaumarchaeota, and this challenges the validity of the SST data, especially for the absolute temperatures.

The dominance of *br*GDGT-Ia is likely the result of degradation of the GDGTs during storage or burial in combination with high *br*GDGT-Ia concentration in the soils. Dominance of *br*GDGT-Ia is known from modern tropical soils, where *br*GDGT-Ia can reach abundances over 95% (Peterse et al., 2012) and suggests climate was characterized by tropical temperatures, soils in the modern dataset with 95% *br*GDGT-Ia have an MAT > 25 ˚C.

The record shows a certain amount of scatter during the PETM (Figure 9), which is likely not a true paleoclimatic signal, even though a sensible explanation for the scatter has not yet been produced, possibly the land derived iGDGTs contribute to this scatter. The Frieling calibration improves the SST record at Margaret Point (Frieling, unpublished results), i.e. it removes the large amount of scatter in the $TEX_{86}^{H}$-based SST, and is coherent with the MBT/CBT-based MAT record of Margaret Point. This new calibration improves the Latrobe-1 $TEX_{86}^{H}$-SST record by removing some of its scatter, although it shows a less prominent warming during the PETM and EECO.

Despite the problems with the SST records, the general trend in the SST records of the Latrobe-1 core, both $TEX_{86}^{H}$-based and the Frieling calibration, show a large similarity with the SST record of ODP Site 1172 at the East Tasman Plateau (Figure 13), which includes a sudden temperature rise during the PETM, a decrease in SSTs just after the PETM, and a subsequent gradual rise to PETM range temperatures during the Early Eocene. Possibly the temperature dependent $TEX_{86}^{H}$ signature of the Thaumarchaeotal GDGTs is still present, despite the land-derived *i*GDGTs in the GDGT-records, or the non-Thaumarcheotal '$TEX_{86}$' (in inverted commas as this index was designed for marine Thaumarchaeotal GDGTs (Schouten et al., 2013)) values of terrestrial origin contain a temperature dependent relationship which is reflected in the increased temperatures during the PETM and EECO.

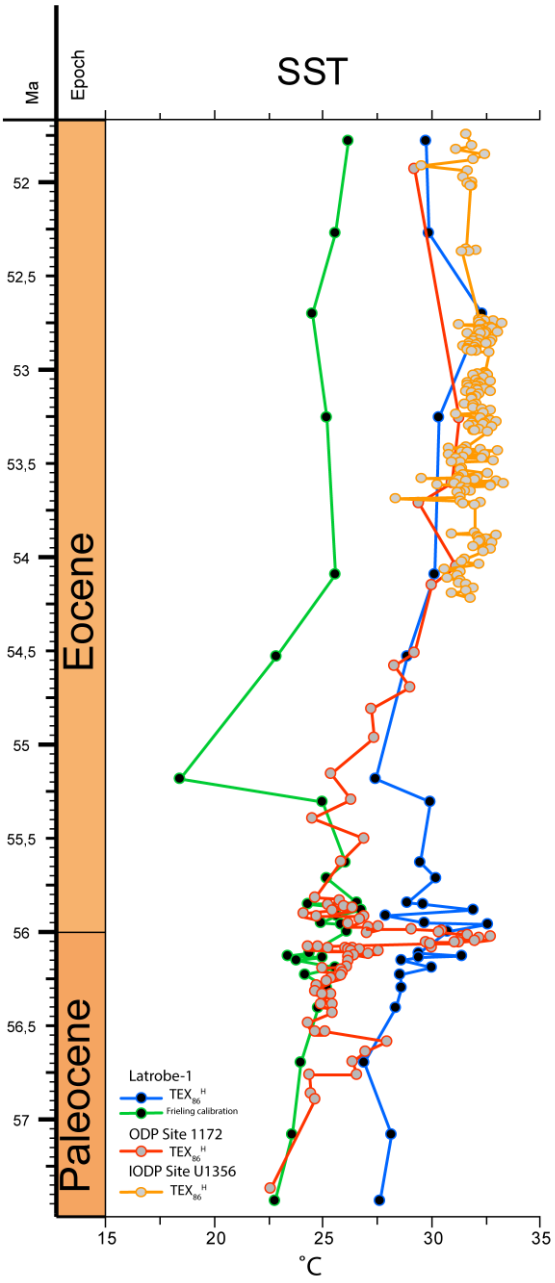


***Figure 13.*** *Plot of the $TEX_{86}^{H}$ SST of the Latrobe-1, ODP Site 1172 (Bijl et al., 2009) and IODP Site U1356 (Bijl et al., 2013) and the Frieling calibration SST of the Latrobe-1 core.*

### 4.3.2 Comparisons of the $TEX_{86}^{H}$ SST records

Comparisons between sites are complicated by the aforementioned problems with the Latrobe-1 SST record. If the SST records of the Latrobe-1 tracks the general SST evolution of the northern AAG, one major difference between the $TEX_{86}^{H}$ SST record of the Latrobe-1 and ODP Site 1172 can be observed, namely that the latter one shows lower 'background', i.e Late Paleocene and earliest Eocene, temperatures than Latrobe-1, while during the PETM and towards the EECO the SSTs are very similar (Figure 13). Low latitude waters brought by the Proto-Leeuwin current possibly kept the AAG warmer compared to the ETP during relatively colder times in global climate. During the PETM and EECO, the west Antarctic margin and Tasman current possibly experienced temperatures that were high enough to have similar temperatures in the AAG and east of Tasmania. Alternatively, a change in ocean circulation, i.e. a change from influence of the Tasman current to influence of the East Australian current, was more pronounced during these high global temperature times.

The Latrobe-1 record and ODP Site 1172 record converge in absolute temperatures at ~54.5 Ma and

the $TEX_{86}^{H}$ record of IODP Site U1356 from ~54 Ma shows similar, i.e. slightly higher but within the 2.5 ° C calibration error, temperatures to these two records (Figure 13). This implies that there are no large regional temperature differences in the AAG and southwest Pacific ocean from ~54 -51.5 Ma.

### 4.3.3 Discrepancies between Sea surface temperatures and terrestrial records

One of the large problems in the Southwest Pacific region and the AAG is the discrepancies in absolute temperatures within SST records reconstructed by the varying proxies and between SST records and terrestrial records (e.g. Hollis et al., 2012; Pancost et al., 2013). Several factors can contribute to the discrepancies between marine and terrestrial proxy records.

$TEX_{86}$ SST records can be too high because of a seasonal bias, especially at high latitudes, as the export of GDGTs to the sea-floor occurs during spring and summer (Schouten et al., 2013). MAT records based on NLRs can be underestimated because of their comparison with modern vegetation, which possibly have 'colder' ranges than in the warmer Eocene; Eocene plant fossils might have no modern equivalent. The modern calibration of soil GDGT does not include soils with temperatures >27 °C (de Jonge et al., 2015), and will underestimate the MAT especially when the GDGT-distribution will be almost solely represented by *br*GDGT-Ia (Inglis et al., 2017). This presents difficulties in comparing terrestrial records with marine records in terms of absolute temperatures.

Similar discrepancies and comparing difficulties between higher temperature $TEX_{86}$ SST records and lower temperature Mg/Ca records are known from New Zealand (Hollis et al., 2012; Hines et al., 2017), and there is ongoing debate if there is an under- or overestimation of temperature for the different proxies and which part of the water column the proxies represent (Ho & Laepple, 2016).

These difficulties and uncertainties in absolute temperatures makes it crucial to look at the biotic response on temperature, either in vegetation or dinocyst assemblages. The following section, the paleoenvironmental reconstruction and integration with regional records, will therefore focus on biotic responses rather than absolute temperatures.

### 4.4.1 Late Paleocene – Early Eocene paleoenvironmental reconstruction and integration with other records

The palynomorph record allows for the reconstruction of the vegetation history in the Eastern Otway Basin based on the nearest living relatives (NLR) of the individual spores and pollen species, while dinocyst assemblages can be used as proxy in paleoclimatic reconstructions, as variability in ecology is reflected in dinoflagellate assemblages (Sluijs et al., 2005; Frieling, 2016).

Vegetation is only one component of the sporomorph assemblage, as factors like basin type, dispersal tactics of the individual plant and spatial distribution of the vegetation will contribute. In a marginal marine setting, the assemblages will be especially affected by sea level and hydrological conditions on land. The Neves effect, the tendency that buoyant sporomorphs (mostly saccate pollen) are overrepresented in their relative abundances in a more distal environment, could potentially influence the assemblages. The fact that there is no large variability in relative abundances of saccate pollen (Figure 10) suggests that there is only minor influence of Neves effect and that large sea-level fluctuations in the studied section are unlikely. The consistent presence of dinoflaggelate cysts indicate that the sediments of the studied samples were deposited in a marine environment; no evidence suggests that deposition was ever fully terrestrial.

This section will first describe the paleoenvironmental reconstruction for the Latrobe-1 core per relevant time interval in the Late Paleocene - Early Eocene. The findings will then be integrated into the regional, i.e. the AAG and the southwest Pacific Ocean, framework as well as compared to the global paleoclimate.

### 4.4.1 Late Paleocene (57.2-56.2 Ma)

#### *4.4.1.1 Latrobe-1*

Late Paleocene (57.2-56.2 Ma; ~370-310 m) vegetation in the Otway Basin, reconstructed from palynomorphs of the Latrobe-1 core, comprises of conifer-dominated rainforest taxa, mainly represented by *Agathis and Araucaria* trees, and minor Podocarpus and *Lagarostrobos*. Smaller vegetation components include ferns, *Gleicheniaceae* (ground ferns) and *Cyathea* (tree ferns) species being the most common. Paleovegetation in the 57.2 to 56.2 Ma interval shows only minor variation, although several angiosperm groups slightly increase towards the latest Paleocene, possibly the result of slight 'background' warming towards the PETM.

Late Paleocene dinocyst assemblages are mostly dominated by species of the *Senegalinium* complex (Figure 11 & 14), a low-salinity tolerant group, suggesting a close proximity to the shoreline. Moreover, the complex likely belongs to the heterotrophic dinoflaggelates (Sluijs et al., 2005), suggesting high nutrient availability in the surface waters. The marine generalist *Spiniferites* complex is also consistently present in the Late Paleocene. Only small amounts of dinocysts have been recovered from the lowermost Pebble Point samples, possibly because of the shallow marine nature of the sediments, and they mainly consist of *Spiniferites* complex, *Senegalinium* complex and small amount of protoperidinoids. After the transgression from the shallow marine Pebble Point formation to the pro-delta Pember mudstone, *Diphyes* becomes an important part of the assemblage, especially pronounced at ~323 m where the species blooms, together with *Senegalinium* complex. Not much is known of the ecology of *Diphyes*, but the *Senegalinium* abundances indicates an environment with significant riverine input.

#### *4.4.1.2 Integration with regional records*

The Late Paleocene vegetation record from the Latrobe-1 core covers the latest stage of the transition from microthermal/mesothermal Podocarp dominated (*Lagostrobos* and *Dacrydinium/Podocarpus*) swamp forests in the Danian and early Thanetian, towards *Araucariaceae/Agathis* dominated rainforests with ferns represented by *Gleicheniaceae* and *Cyatheaceae* which has been documented in coastal lowlands of Southeast Australia (Macphail et al., 1994). Late Paleocene southeastern Australian vegetation is similar to the reconstructed vegetation at the East Tasman Plateau after the Middle/Late Paleocene transition (Contreras et al., 2013), i.e. large similarity in species and minor differences in relative abundances, including higher abundances of *Cyatheaceae* and lower abundances of *Dilwynites* at the ETP.

Although only small amounts of dinocysts have been recovered from the lowermost Pebble Point samples, the dominance of protoperidinoids and other peridinoid dinocysts closely resemble the microplankton of Pebble Point outcrops (Cookson & Eisenack, 1965), congruent with a shallow marine depositional environment. Oxygen isotope data of two different species of Cephalopods found in the Pebble point outcrops

yielded paleotemperature estimates of 18-25 °C (Ward et al., 2016), which is within the range of the $TEX_{86}^{H}$ data of the Latrobe-1.

The Pebble point transgression, which facilitated a change from the shoreface deposits of the Pebble Point Fm. to the pro-delta deposits of the Pember mudstone, is a Late Paleocene transgression which has been documented in the AAG (e.g. McGowran et al., 2004), as well as in the Gippsland basin, therein named the *Apectodinium reburrus* transgression (Partridge, 1999), after the epynomous dinocyst associated with the marine incursion.

### 4.4.2 PETM: onset to recovery (56.2-55.8 Ma)

*4.4.2.1 Latrobe-1*

During the latest Paleocene (~310 m) about 5-10 meters below the PETM, a decrease in *Senegalinium* complex and *Delfandrea/Cerodinium* species is observed, concomitant with an increase in *Glaphyrocysta*, both in relative abundances and concentration (Figure 11), which suggest a transgression and movement away from low salinity conditions. In the same interval, an increase in the *Paralecaniella*/dinocysts ratio is observed (data not shown), believed to reflect high hydrodynamic (stressed) environments (Louwye & Laga, 2008; Brinkhuis & Schiøler, 1996), consistent with a transgression. The transgression is accompanied by a sudden change in vegetation, demonstrated by an increase in angiosperm *Proteaceae* and *Arecaceae* (Palm) pollen and fern spores of *Gleicheniaceae* and *Laevigatisporites* (?*Blechnaceae*), with a subsequent decrease in the conifer taxa *Agathis* and *Araucariaceae*, both observed in the relative abundances, as well as the absolute concentrations. The increase in angiosperm pollen with mesothermal-megathermal affinities (e.g. *Arecaceae*) indicate Late Paleocene warming that culminated into the PETM. The increase in fern spores (from a Late Paleocene average of 15% up to 40%), are indicative of a disturbed ecosystem, ferns being opportunistic species that thrive well in disturbed ecosystems. The fern spores are mainly represented by *Gleicheniaceae* and *Blechnaceae,* which suggests a change to a relatively open, perhaps swampy and/or highly disturbed sites edging the water (Carpenter et al., 2004). The disturbance of the ecosystem could be induced by warming but more likely reflects a change from rainforest to more swamp type vegetation at the coastal plain, as a result of the transgression that occurred in this interval and/or intensifying of the hydrological cycle. The discussed change in vegetation precedes the lowest $\delta^{13}C$ values of the PETM and even precedes the first decrease in $\delta^{13}C$ values (position 1 in Figure 12) by ~2 meters. This indicates that the shift in vegetation type and the transgression precedes the PETM by several 10s of kyrs (based on 5 cm/kyr sed. rate; see section 3.1) or reflects the initial stages of PETM warming if the interval is relatively expanded.

The *Glaphyrocysta* dominated interval is followed by an increase in *Senegalinium* species and the first peak (~25%) in *Apectodinium* (mainly *A. hyperacanthum*) is recorded, coincidental with the first decrease in $\delta^{13}C$ values (Figure 11). The migration of *Apectodinium,* which is confined to the tropics in the Paleocene, to the Northern AAG at the PETM onset reveals the PETM warming. The increase in *Senegalinium* species suggest that low salinities and probable increased supply of nutrients prevailed in this interval, possibly by an increased terrestrial hydrological cycle in response to warming.

At peak-PETM conditions, marine palynomorphs reach their maximum extent of 50% of the total assemblage, with a dominance of *Apectodinium* spp. (mainly *A. homomorphum*). The increase in the ratio of marine palynomorphs seems primarily the result of the increase of *Apectodinium* concentration, as the concentration of other dinocyst groups remain stable or decrease and total terrestrial palynomorph concentration increases in that interval (Figure 9), suggesting optimal

conditions for *Apectodinium* growth, i.e. near-tropical temperatures in the northern AAG during the PETM. Apectodinium requires minimum temperatures of ~20 °C (Frieling et al., 2014) and the optimal temperatures of >25 °C (Frieling, 2016) During the same interval the first occurrence of the tropical mangrove palm *Nypa* (minimum MAT > 24°C) is recorded. This occurrence, together with *Intratriporopollenites notabilis* (*Brownlowia* (Macphail, 2007), is the first indicator of megatherm (MAT >24 °C) vegetation, as well as first indicators for mangrove coastal vegetation. *Euphorbiaceae* (*Malvacipolis* spp.) are first recorded from the PETM and continue to be consistently recorded in the Early Eocene as a minor component of the assemblage (< 10%). The increase of fern and angiosperm pollen during the PETM could be solely the result of an intensifying of the hydrological cycle, which would allow greater transport of the relatively small fern and angiosperm pollen and thereby increasing their diversity and abundance. Although this possibly plays a role in the composition of the assemblage, it is not likely this is the only contributing factor. Especially when considering that the total sum of pollen actually decreases at the onset of the PETM, and only increases again during the recovery (Figure 9). Furthermore, the persistence of these angiosperm pollen in the Early Eocene and the introduction of megathermal elements during the PETM substantiate a true vegetation signal.

During the PETM recovery, ferns and angiosperm *Proteaceae* decrease toward pre-PETM abundances, while *Agathis* shows the opposite trend. The Earliest Eocene interval (~295-280 m) shows a large similarity in vegetation to the Late Paleocene interval prior to the PETM onset, except for a larger diversity in angiosperms. *Malvacipolis*, *Ericipites*, *Arecipites*, *Tricolpites* and *Tricolporate* spp. all occurred first around the PETM and are minor components during the Earliest Eocene.

Overal dinocyst concentrations in this interval decrease and assemblages are dominated by *Spiniferites* complex. The decrease in P/G ratio, dominance of autotroph species, likely reflects a shift in nutrients. possibly as a result of a decrease in the terrestrial hydrological cycle during post-PETM cooling; P/G ratio decreases towards pre-PETM values. Alternatively, the high *Spiniferites* interval corresponds to a maximum flooding surface at the end of the PETM. This potentially results in the same P/G ratio trend; the observed change is probably a combination of these two factors.

The discussed changes in vegetation and dinocysts show that the warming that culminated in the PETM had a profound influence on paleoenvironment in the Eastern Otway Basin. Vegetation changes precede the onset of the PETM, possibly as a result of disturbance of the coastal ecosystem by the transgression. During Peak-PETM conditions, vegetation and the *Apectodinium* acme reveals the tropical temperatures that prevailed during the PETM. The subsequent post-PETM shift in vegetation towards assemblages that resemble the Late Paleocene and the disappearance of *Apectodinium* shows that the environment was 'recovered' in less than ~200 kyrs. Late Paleocene flora with a preference for mesic conditions possibly found their refuge at higher altitudes during the PETM and migrated back to coastal areas as a response to post-PETM cooling. The PETM (including the onset) introduced several genera of angiosperms that, although as a minor component at first, are consistently recorded throughout the whole Early Eocene.

*4.4.2.2 Integration with regional records*

Transgression associated with or just before the PETM has been observed in many parts of the world, calling to the global nature of the transgression (Sluijs et al., 2008b). The transgression in the AAG has been recorded in the Otway basin and adjacent basins (e.g. this study; Taylor et al 1964), the Torquay (sub-)basin (Holdgate & Clarke, 2000; Holdgate et al., 2001), the Bass basin (Partridge, 2002; Briguglio et al., 2013) and the Sorell basin (Boreham et al., 2002). West of the Tasman sills, the transgressions has been observed at the ETP (ODP Site 1172; Sluijs et al., 2011) and north of

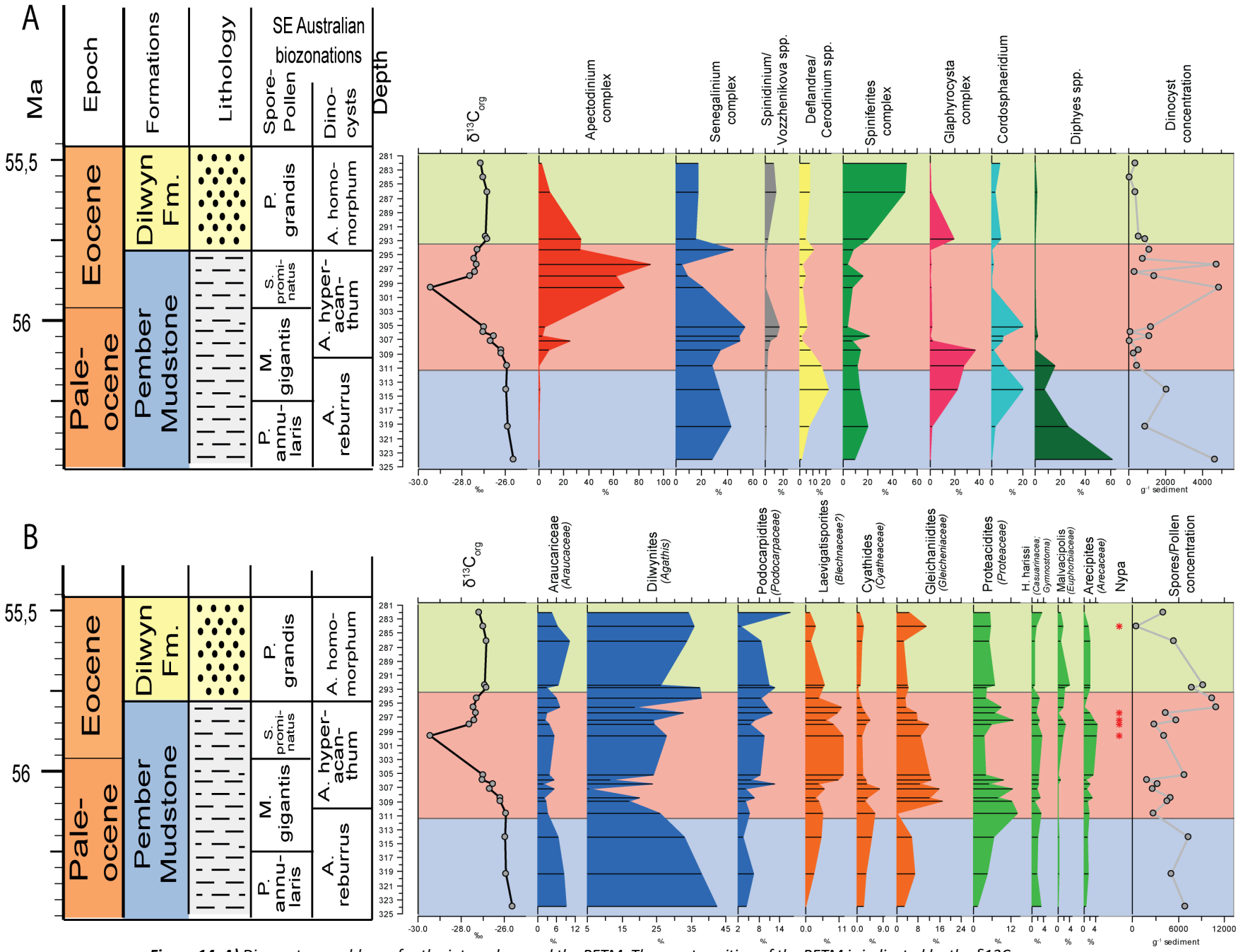


***Figure 14. A)*** *Dinocyst assemblages for the interval around the PETM. The exact position of the PETM is indicated by the δ13C values.* ***B)*** *Spore Pollen assemblages for the PETM interval.*

Tasmania in the Gippsland basin (Partridge, 1999), as well as different locations in New Zealand (e.g. Handley et al., 2011; Pole et al., 2010).

The latest Paleocene transgression facilitated the shift of coastal lowland forest to swamp-type vegetation and the deposition of coal in the Torquay basin (Holdgate et al., 2001), a potential source area for terrestrial sporomorphs in marine Otway basin sediments. The initial floral changes at the (pre-) onset of the PETM, i.e. increase in ferns at the expense of gymnosperms, are probably result of disturbance of the coastal ecosystem in the Eastern Otway basin rather than temperature, as the megathermal elements are not present until peak-PETM. Similar changes in flora during the PETM transgression is observed in New Zealand (Handley et al., 2011), although increase in swamp vegetation and megathermal elements are more or less simultaneous there.

The appearance of megathermal elements, e.g. the mangrove palm *Nypa*, is observed at almost every site in southeast Australia, including the Otway basin, the Bass basin (Partridge, 2002), western Tasmania (Macphail, 2013) and the ETP (Contreras et al., 2013), as well as in New Zealand (Handley et al., 2011; Pole et al., 2010), although relative abundances vary as a result of the proximity to the source. The ubiquitous, although transient, presence of megathermal elements in this high latitude region during the PETM underline the flat meridional temperature gradient during this hyperthermal. The PETM facilitated a rapid shift in plant community observed throughout whole Australia (Macphail et al., 1994).

At the ETP megathermal elements appear during the PETM, while pollen with long transport capacity (*Dilwynites* spp.) increase, reflecting the transgression and consequent shift to a more distal environment (Contreras et al., 2013). The exact opposite trend in *Dilwynites* and other gymnosperm pollen for the Latrobe-1 core can be attributed to difference in initial source proximity. Although transgression took place in the northern AAG, the environment did not become sufficiently distal to be reflected in the sporomorph record. On the contrary, the sporomorph record became enriched in 'harder' to transport angiosperm and fern pollen, presumably due to enhancement of the hydrological cycle and/or reorganization of the terrestrial vegetation.

Dinocyst records of the PETM at the ETP show similarities with Latrobe-1 in several aspects. The first abundant appearance of tropical *Apectodinium* is recorded just below the PETM, following a *Senegalinium* dominated latest Paleocene interval (Sluijs et al., 2011). *Glaphyrocysta* becomes abundant just before the first *Apectodinium* peak, similar to the Latrobe-1 dinocyst record. The two similar trends indicate first transgression, and subsequent or concomitant migration of tropical dinocysts to higher latitudes prior to the PETM. Only very slight warming (~1 °C) preceeds the CIE in $TEX_{86}^{H}$ records at the ETP (Sluijs et al., 2011), and $TEX_{86}^{H}$ and MBT/CBT at Margaret Point, northern AAG (Frieling, unpublished results), signaling that temperature was perhaps not the most important driver of the migration of *Apectodinium* to these regions. The anomalous pre-PETM *Apectodinium* abundance could reflect the early stages of PETM warming if these deposits were relatively expanded (Sluijs et al., 2011). This explanation has also been proposed for the initial $\delta^{13}C$ step in both the Latrobe-1 and Margaret Point (see section 4.2), which coincides with the first *Apectodinium* abundance at these site, although this $\delta^{13}C$ step is less prominent, if present at all, at ODP Site 1172.

While in the Latrobe-1 *Apectodinium* abundance reach 60-80% during peak-PETM, *Apectodinium* at Site 1172 is relatively small (20-30%). Instead, at Site 1172, several other dinocysts groups (e.g. *Pyxidinopsis, Eocladopyxis* and *Membranosphaera*) show mutually separate peaks throughout the PETM, which are not found in the Latrobe-1. Presence of *Pyxidinopsis*, an Antarctic endemic species, at the ETP is expected because of the influence of the Tasman current, which did not flow into the northern AAG. The presence of *Eocladopyxis* at Site 1172 is related to high salinity and perhaps

storminess (Sluijs et al., 2011). These high salinities were probably not established at Latrobe-1, due to the high freshwater input.

The paleoenvironments during the PETM between the northern AAG and ODP Site 1172 seem very similar in regard to temperature, reflected in both vegetation and dinocyst records. Therefore the difference in the paleoceanographic currents, i.e. influence of low- vs. high latitude waters, did not cause a large temperature difference in the PETM, possibly because of the large magnitude of warming at the poless and/or a decreased influence of the Tasman current during this event.

### 4.4.3 Earliest Eocene (55.8-53.4 Ma)

#### *4.4.3.1 Latrobe-1*

The lower sampling resolution in the Early Eocene interval does not allow a high resolution vegetational history, but general long term trends and paleoenvironmental reconstructions can be inferred. The earliest Eocene vegetation (*Proteacidites grandis* zone; 55.8-54.5 Ma) shows large similarities with the former described Late Paleocene and post-PETM vegetation, with a very large dominance of the conifer rainforest taxa *Agathis*, *Araucaria* and *Podocarps* and low angiosperm diversity (see Appendix 5).

In the Early Eocene, the marine palynomorph ratio decreases and dinocyst concentrations are not sufficient for analysis; little information can be extracted from the dinocysts in the 280-160 m interval. The change in depositional environment likely played a role in the decrease of marine palynomorphs. From the Early Eocene a series of deltaic cycles are deposited, consisting of large sandstone deposits interchanged with finer mud and siltstones; the nearshore and high energy environment that facilitated these deposits where probably not optimal for dinoflaggelate habitation. The encountered dinocysts are mainly from the *Spiniferites* complex and *Senegalinium* complex in this interval.

During the *Proteacidites tuberculiformis* zone (54.5-53.4 Ma), the conifer rainforest taxa decline, while angiosperms of *Proteaceae, Casuarinaceae, Euphorbiaceae* and *Nothofagus* all show an increase, marking the beginning of the angiosperm dominance (relative abundance >50%). Furthermore, a large rise in the number of angiosperm species in this interval is recorded (from ~15 to ~25 species; see Appendix 5). The rise of the angiosperms at the expense of gymnosperms is a phenomenon that has been recorded in many parts of the world during the Cretaceous and Cenozoic. Explanations of the mechanisms of this floral overturn include better adaptations of angiosperms to dryer climate, an advantage over gymnosperms when nutrient availability is high, the ability to grow faster, the development of features that provide advantage in biotic interactions, and the production of new lineages by an increased rate of phylogenetic branching with the potential to occupy particular niches (Augusto et al., 2014). Most of these explanations likely played a role, but their relative importance varied over space and time, creating difficulties explaining the angiosperm rise in this part of the Otway Basin. The introduction of new angiosperm genera and species has been observed for the PETM, suggesting that the paleoenvironmental change during that interval was suitable for angiosperms, probably occupying a niche that arose as a consequence of warming, changes in the hydrological cycle or changes in the coastal ecosystem. Providing that the PETM had this effect on angiosperms, it is probable that other Eocene hyperthermals, e.g. the ETM-2 /H1/Elmo(~54 Ma; Lauretano et al., 2016), had a similar effect. Based on its timing, the ETM-2 should be located in the *Proteacidites tuberculiformis* zone (54.5-53.4 Ma), whereas the angiosperm rise is

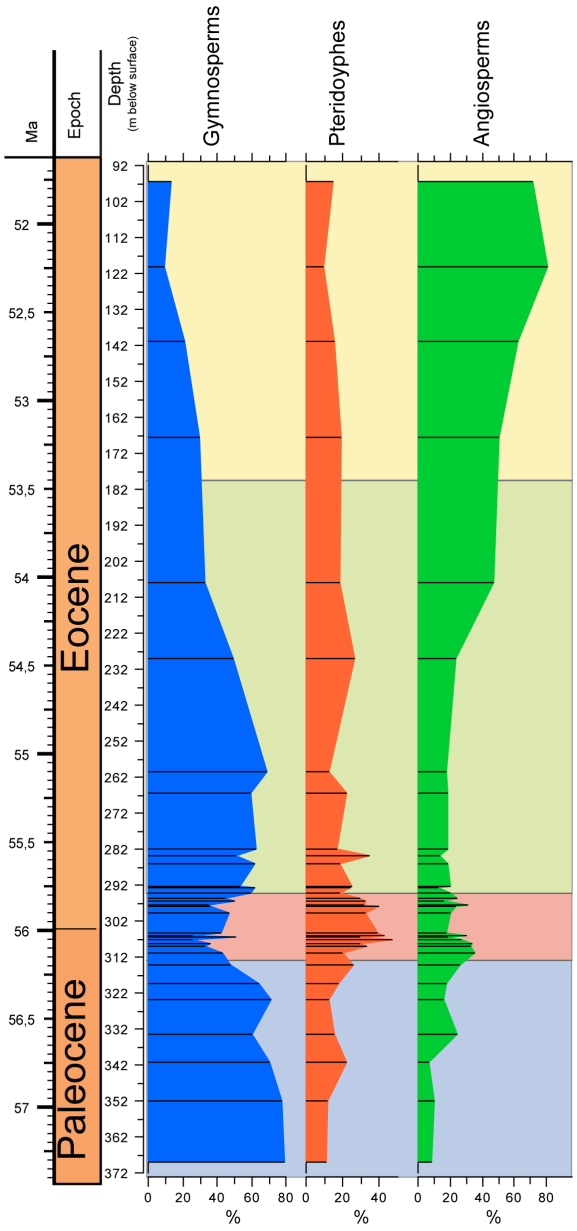


***Figure 15.*** *Relative abundaces of gymnosperms, pteridophytes and angiosperms throughout the core.*

recorded between the two samples in this interval. These observations suggest a possible link, whether paleoclimatic or taphonomic, between this hyperthermal and angiosperm abundance; higher resolution work on the Early Eocene hyperthermals could shed more light on this suggested link.

*4.4.3.2 Integration with regional records*

The introduction of several angiosperm lineages during the PETM and the Early Eocene is recorded in the Latrobe-1, and are part of the replacement of conifer gymnosperms by angiosperm as the dominant rainforest taxa in the southeastern Australian region. Several of these Early Eocene angiosperm taxa can be related to modern tropical evergreen, nonseasonal and megathermal rainforest (Macphail et al., 1995).

Before these elements get dominant in the Early Eocene, the Latrobe-1 record shows that for the earliest Eocene, i.e. the first ~1 Myr after the PETM, conifer rainforest taxa dominate (similar to Late Paleocene), possibly due to post-PETM cooling shown in temperature records of e.g. the ETP (Bijl et al., 2009). Sporomorph based paleoenvironmental reconstructions of ODP Site 1172 shows a similar response of vegetation at the ETP on the decrease in temperature in the Earliest Eocene (Contreras et al., 2014). In New Zealand records, after the PETM, a consistent dramatic increase in *Casuarinaceae* is observed (e.g. Handley et al., 2011; Pole, 2010). Timing in these records is not precise, but it is estimated that *Casuarinaceae* start to dominate at ~54.5 Ma, possibly as a result of the increase in temperature in that interval (Pancost et al., 2013). While *Casuarinaceae* domination in the Northern AAG is not observed until later in the EECO, angiosperm diversification and increase (mainly *Proteaceae*, *Malvaceae* and unidentified *Tricolpites* spp.) is recorded close to that interval, possibly related to Early Eocene hyperthermals (ETM-2/ELMO). The association of *Casuarinaceae* and the EECO in the Latrobe-1 suggests *Casuarinaceae* thrives well in high-temperature climates. Early Eocene New Zealand was positioned 5-10° to the north of Southeast Australia (van Hinsbergen et al., 2015), and potentially experienced warmer climates relative to Australia earlier in the Early Eocene. *Casuarinaceae* thrive well in low nutrient environments (see section 4.4.4.1), suggesting nutrient availability could have played a role in the difference between Australia and New Zealand. Alternatively, precipitation differences might have contributed to the timing of *Casuarinaceae* domination. Sparsity of data on the previously mentioned factors complicate explaining the differences between Australia and New Zealand.

The sporomorph record of IODP Site U1356 at Wilkes Land on Antarctica (53.9-51.9 Ma) has its base just after the ETM-2/ELMO and the base of this record corresponds to the previous mentioned interval where angiosperm abundances and diversity increase in the Northern AAG. The sporomorph record shows near tropical and winter frost free temperatures for the complete Early Eocene interval studied (Pross et al., 2012), with little variation. Consistent abundance of *Nothofagus* (~20%), represent the more temperate rainforest biomes of the hinterland, while meso-megathermal rainforest vegetation thrived near the coast. The near-tropical temperatures are underlined by the constant abundance of *Apectodinium* (Bijl, unpublished results). *Apectodinium* disappears from the records at the Latrobe-1 in the Early Eocene, only to reappear around ~52.8 possibly near the ETM-3. This interval without *Apectodinium* is presumably deposited very near-shore, and the bulk of the samples are almost barren of dinocysts, with the exception of rare *Spiniferites* and *Senegalinium*. *Apectodinium* is probably, as previously mentioned, the most distal end-member of the Latrobe-1 dinocyst assemblage, which would explain their absence in this interval. Coastal proximity appears to be the limiting factor for *Apectodinium* growth in the AAG, rather than temperature, as a warmer Antarctic coast relative to the northern AAG does not seem very likely because of its lower latitude and the configuration of paleoceanographic currents. Furthermore, *Apectodinium* are found for this interval in adjacent basins in the AAG, e.g. the Bass basin (Partridge, 2002) suggesting temperature is not the limiting factor in the northern AAG. In the Latrobe-1, *Apectodinium* reappears when the ratio of marine palynomorph increases, indicating the depositional environment becomes sufficiently distal.

At the ETP, *Apectodinium* also disappears from the assemblage in the Early Eocene but at that location the environment should be sufficiently distal for *Apectodinium* growth; other encountered dinocysts have an association with offshore environments (Bijl, 2007). This seems to be the result of the influence of the Tasman current derived from west-Antarctica, prohibiting *Apectodinium* growth by decreasing the temperature or another current-specific physical parameter. Lower temperatures are found in sporomorph and plant macrofossil records of the Early Eocene of east Tasmania (Macphail et al., 1995), showing a micro-mesothermal vegetation with abundant Nothofagus, suggesting a high temperature gradient between west and east Tasmania (Macphail, 2007). This underlines the influence on temperatures of the Proto-Leeuwin current and the Tasman current on the AAG and ETP respectively. Further influence by the Tasman current is found in Early Eocene vegetation records in the Bonaparte Basin, Queensland, on the northeastern coast of Australia, where vegetation reflecting slightly lower temperature than southeast Australia is present (Mcphail, 2007). Precise timing of this record is unclear, therefore it remains possible this site is deposited in the 'cold' ~1 Myr after the PETM and therefore temperature differences are minimal.

### 4.4.4 Towards the ETM-3 and EECO (53.4 – 51.7 Ma)

#### *4.4.4.1 Latrobe-1*

Angiosperms remain the dominant element in the *Myrtaceidites tenuis* zone (53.4-51.7 Ma), possibly the result of the continued warming into the EECO. *Casuarinaceae* (*H. harrisii*), known wind-pollinators, become the dominant component during this interval, while the megathermal (mangrove) elements *Nypa* and *Intratriporopollenites notabilis* (*Brownlowia*) return to this part of the Otway Basin, together with the first appearance of *Myrtaceidites tenuis* (primitive Eucalyptus) pollen. Other angiosperm elements consist of *Euphorbiaceae, Proteacea, Tricolporate* spp. and contributions of *Ericaceae*.

At 140 m (~53-52 Ma), dinocyst abundances increase again an a second peak of *Apectodinium* (mainly *A. homomorphum*) can be found, which is its first occurrence in the core since the PETM. The peak coincides with a ~2° C increase in $TEX_{86}^{H}$ SST. The second occurrence of *Apectodinium* reveals Early Eocene warming with temperatures close to the PETM, in harmony with the re-appearance of megathermal pollen elements. Although timing of this peak is not precise because of the lack of resolution, the position of this peak makes it probable it is associated with the ETM-3/K/X event (~52.9 Ma; Lauretano et al., 2016) and possibly marks the begin of the EECO. The *Apectodinium* peak is concomitant with a peak of the mid-shelf genus *Cleistosphaeridium*, which suggest sea level was higher than during the more or less barren dinocyst interval that underlies this sample. *Apectodinium* spp. are probably the most distal end member of the dinocysts encountered in the Latrobe-1.

The second occurrence of megathermal elements reflects the warming that culminated into the EECO, possibly 'punctuated' by Eocene hyperthermals. Present day Australian *Casuarinacea* grow in seasonally dry conditions, although *H. harrisii* pollen are probably related to the modern *Casuarinaceae* genus *Gymnostoma*, the 'rainforest *Casuarinacea*', growing in present day Malaysia. This is based on of the association of *Casuarinaceae* pollen with rainforest elements in Cenozoic Australian sediments, and the presence of *Gymnostoma* macrofossils in contemporary deposits (Macphail et al., 1995; Hill, 1995).

Possibly the rise in angiosperms, and especially *Casuarinaceae*, is linked to the increasing atmospheric $CO_2$ in the Early Eocene, as soil nitrogen is a limiting factor to the increased growth and photosynthetic rates in plants in elevated atmospheric $CO_2$ environments (e.g. Sigurdsson et al., 2013). *Casuarinaceae*, including *Gymnostoma*, are actinorhizal plants(Dawson, 2007), i.e. they contain nitrogen-fixing symbionts within nodules in their root system, and would therefore be less limited by soil nitrogen. Higher rates of growth under elevated $CO_2$ has been shown for at least one species of modern *Casuarinaceae* (Karthikeyan, 2016) *Casuarinaceae* are the only extant actinorhizal plants of Gondwanan origin (Dawson, 2007), which could explain their dominance in Australia and New Zealand during the Early Eocene, especially when nutrient availability is limited. Several modern day *Casuarinacea* are salt-tolerant and can live on sandy soils (Ngom et al., 2016), and are therefore suited to live near the coast, possibly in association with the mangrove vegetation. Proteaceae plants, which are moderately abundant during the EECO, also have a tolerance to low nutrient environments, supporting the idea of low-nutrient soils on the southeastern coast of Australia during the EECO.

Dinocyst assemblage in the youngest sample (~51.7 Ma) of the core are dominated by *Homotryblium tasmaniense*, the first account of significant amounts of epicystal goniodomids in the core. *Homotryblium* spp. are associated with high temperatures, polysalinity and possibly restricted marine/lagoonal environment (Sluijs et al., 2005). While records from the EECO and PETM yield similar temperatures, in this study and at the ETP (Bijl et al., 2009), and also reflected in the deep-sea benthic $\delta^{18}O$ values in the two periods (Zachos et al., 2008), the paleoenvironment in the northern AAG was not that similar. This is partly reflected in vegetation, from the PETM towards the EECO there is a rise in angiosperms at the expense of gymnosperms and ferns. Dinocysts of Late Paleocene and PETM show dominance of low salinity P-cysts and *Apectodinium*, while in the EECO p-cysts are almost completely absent. This implies a lack in supply of nutrients in the EECO, possibly because of less riverine input, underlined by the lack of low-salinity tolerant dinocysts. Therefore it seems the intensification of the hydrological cycle that is recorded in the PETM, is not apparent in part of the EECO, or possibly, the precipitation regime had a strong seasonal component.

The sporomorph based vegetation reconstruction of the Northern AAG throughout this part of the Early Eocene (53.4-51.7 Ma), partially including the warmest period of the Cenozoic (EECO), is dominated by rainforest non-seasonal megathermal elements at ~55° S paleolatitude, comparable to PETM temperatures in Southeast Australia and modern day tropics.

*4.4.4.2 Integration with regional records*

After ~53.4 Ma mangroves with megathermal elements (*Nypa*) reappear again at the northern AAG, in the Eastern Otway basin as well as in the Bass basin (Partridge, 2002) and Gippsland basin (Partridge, 1999), presumably as the result of the Early Eocene warming trend culminating in the EECO. The presence of megathermal elements in the northeastern AAG and their absence on the Wilkes land margin (Pross et al., 2012) show that the temperature gradient between the northern and southern margin of the AAG is reflected in the vegetation. There are several differences in Early Eocene vegetation between the northern and southern margin of the AAG. High abundances of *Nothofagus* (avg. ~20%) and *Cyathecaeae* (avg. ~40%) are found at Wilkes land, where they are almost completely absent in the Latrobe-1, while the high abundance of *Casuarinaceae* on the northern margin of the AAG is not recorded at Wilkes Land (Pross et al., 2012). This shows that there was a large difference in the dominant components of vegetation at on the one hand south Australia, Tasmania and New Zealand (which have very similar compositions), and Antarctica. This is underlined by the occurrence of taxa at Wilkes Land that disappeared in southern Australia in the Paleocene (e.g. Gambierina edwardsii), which probably survived on the Antarctic continent. Carpenter et al., 2014) is the southernmost extent of megathermal elements during the Early Eocene. Coexistence approach applied to western Tasmania sporomorphs reveal MATs of at least 24° C (Carpenter et al., 2014), assemblages of the Latrobe-1 are very similar. Wilkes Land the MAT reconstructed using MBT/CBT reveal temperatures around 25° C (Pross et al., 2012), indicating MAT in northern AAG probably exceeded 25° C.

Early Eocene deposits in New Zealand also contain the megathermal Nypa (e.g. Pocknall, 1990), and an increase in $TEX_{86}^{H}$ SST from ~53 Ma, towards values of 32° C (Hollis et al., 2009) is recorded, concomitant with a slight increase in warm water nannofossil taxa, although these rather represent warm-temperate temperatures, instead of recorded (sub-) tropical (Shepherd, 2017). This indicates that there was no (large) temperature gradient from SE Australia to on a slightly more northern latitude located New Zealand. SST records in a roughly north-south transect off the east coast of (paleo-) New Zealand shows no meridional temperature gradient over ~10° latitude (Hines et al., 2017). The low meridional gradient together with the low vertical temperature gradient in the water column during the EECO in New Zealand suggests that surface currents had a large influence during the EECO (Hines et al., 2017). High resolution $\delta^{13}C$ records from two sites at Mead Stream, New Zealand, expose several Eocene hyperthermals, from the PETM to the EECO (Slotnick et al., 2012; Slotnick et al., 2015). High terrestrial weathering linked to the hyperthermals, most pronounced in the ETM-2 and ETM-3/K/X event. Furthermore, the high resolution records show a negative step in $\delta^{13}C$ values and gradual decrease from the J event (~53.35 Ma) towards the CIE of the ETM-3 (~52.9). This step and decrease coincides with the start of the M. tenuis biozone and the reappearance of megathermal elements (e.g. Nypa) in SE Australian basins (Partridge, 1999; 2006) including in Latrobe-1. This indicates that from ~53.4 $CO_2$ became sufficiently high for 'PETM-like' temperatures and this seems to mark the start of the EECO in the region.

Although the EECO and PETM experienced similar temperatures, sporomorph records in the Latrobe-1 show large differences in dinocyst and vegetation records. Vegetation was almost

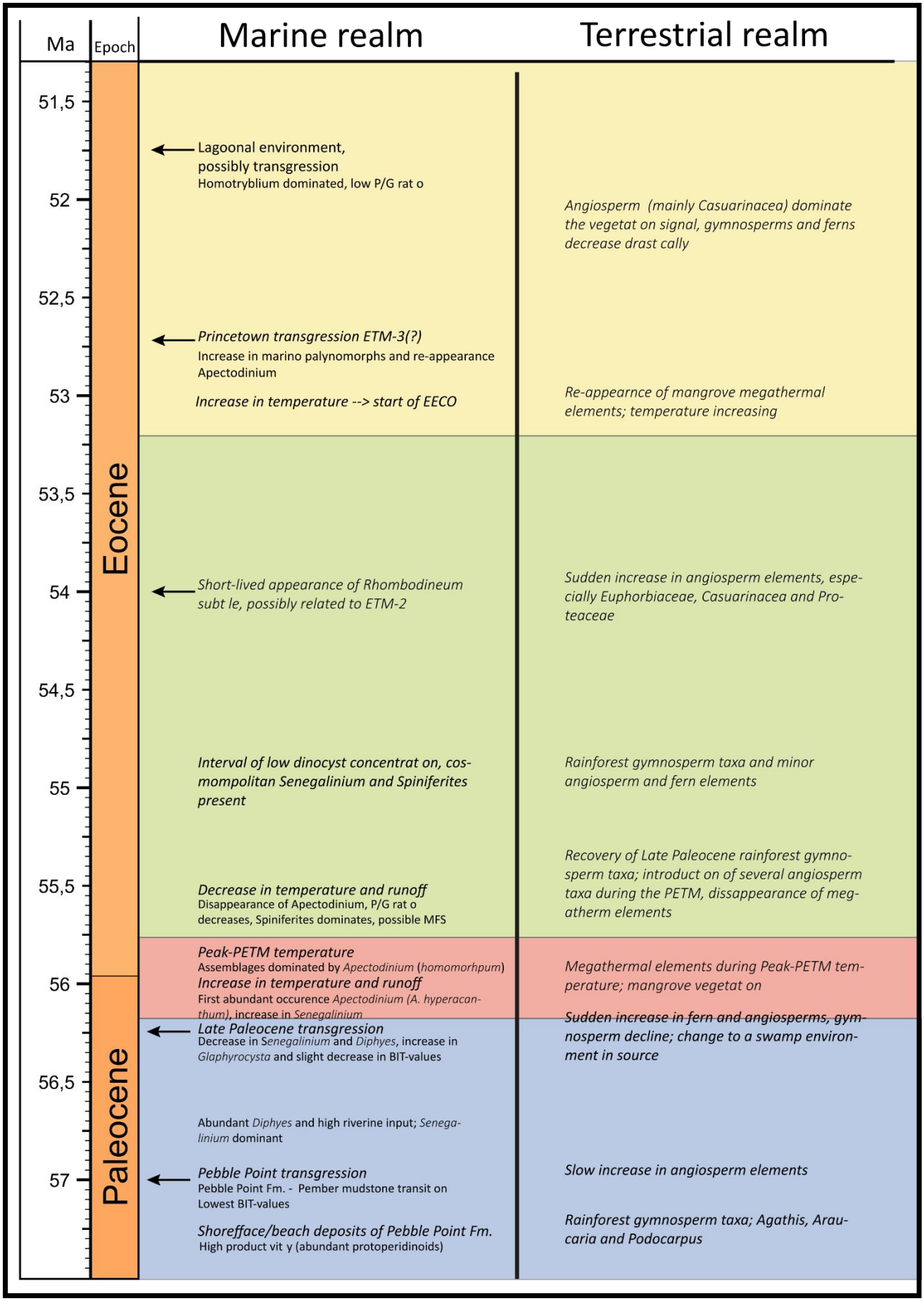


***Figure 16.*** *Table showing the important events in the Late Paleocene – Early Eocene interval for the Latrobe-1. Color shadings show the relevant time periods, including Late Paleocene (blue), PETM (red), early Eocene (green) and EECO (yellow).*

completely dominated by angiosperms, instead of Late Paleocene/ PETM conifer rainforest taxa. fThese vegetation changes have been recorded throughout the whole of SE Australia (Macphail et al., 1995), indicating this is not a local phenomenon.

The largest difference in dinocyst assemblages between the Late Paleocene and Early Eocene is the widespread occurrences of epicystal goniodomids, mostly in the form of Homotryblium tasmaniense; in the Latrobe-1, Tasmania (Carpenter et al., 2012), Wilkes Land (Bijl, unpublished results), Mid-Waipara river (Hollis et al., 2009) and ODP Site 1172 (Bijl, 2007). Goniodomids are probably related to modern Polyshaeridium zoharyi (Fensome et al., 1993), which are associated with hyperstratification and lagoonal conditions in the ocean (Reichart et al., 2004), possibly due to a net evaporation budget. The widespread occurrence of these dinocysts on sites outside the coastal realm could indicate that large parts of Early Eocene shelfs were very shallow. Although not much is known of the ecology of these dinocysts, they seem to flourish well in places with changing salinity (Wall et al., 1977). Possibly the EECO had a seasonal component in the climate in contrast to the non-seasonal Late Paleocene- Earliest Eocene climate causing varying salinity in near coastal and possibly open ocean sites.

**4.5 Integration with the global paleoclimate**

The Late Paleocene to Early Eocene encompass the global warming trend from the mid-Paleocene towards the EECO, comprising the warmest sustained temperatures of the last 65 Myr. The warming trend was punctuated by several hyperthermals, all associated with light carbon injection into the atmosphere (Lauretano et al., 2016), and of which the PETM is the most pronounced. The PETM has been extensively studied, in continental and marine settings, from the northern to southern high latitudes. The Latrobe-1 PETM shows similarities with the global records, which include a ~5° C warming relative to the Late Paleocene, a Late Paleocene transgression and the *Apectodinium* acme in coastal shelf settings. Almost every terrestrial PETM site around the world shows a change in floral composition during the hyperthermal, although the magnitude and type of change varies widely (Wing & Currano, 2013). The high SST , as well as the appearance of megathermal elements at Latrobe-1 and in the region confirm a low meridional temperature gradient. High temperatures at high latitudes have also been shown for the Arctic (e.g. Sluijs et al., 2006), while extremely warm temperatures are recorded near the equator (Frieling et al., 2017) during the PETM. The PETM recovery at the Latrobe-1, i.e. return to to background (although slightly more negative than Paleocene) $\delta^{13}C$ values, return to vegetation similar to the Late Paleocene and last occurence of *A. hyperacanthum*, was established in ~200 kyr after the start of the PETM, more or less the estimate of global duration of the PETM (McInerney and Wing, 2011).

The exact location of other Eocene hypterthermals in the Latrobe-1 is problematic because of lack of carbon isotope data, although biostratigraphic data implies that several of these hyperthermals can be found in the core. The ETM-2 (~54 Ma), the first major hyperthermal after the PETM, is considerably less known in terms of paleoclimatic and biotic changes, although records of the Arctic suggest warm and wet conditions during this hyperthermal (Sluijs et al., 2006; Suan et al., 2017) at high latitudes, similar to the PETM.

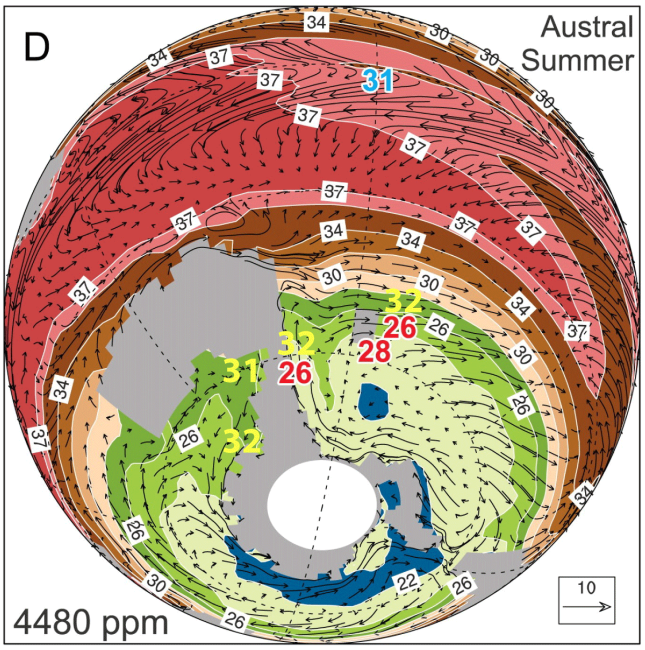


***Figure 17.*** *Comparisons of model data at 4480 ppm $CO_2$ from Hollis et al., (2012) with proxy SST records of the AAG and southwest Pacific for the EECO. Red numbers: $TEX_{86}^{L}$ SST data from ODP Site 1172, Hampden beach and Mid-Waipara (Hollis et al., 2012). Yellow numbers: $TEX_{86}^{H}$ of the Latrobe-1 and Wilkes Land in the AAG, $TEX_{86}^{H}$ of ODP Site and Mid-Waipara displayed above the $TEX_{86}^{L}$ value of the same location. Modified after Hollis et al. (2012).*

EECO records from the southwest Pacific and the AAG show similar temperatures as during the PETM. The high temperatures at the northern AAG seems to not completely fit with modeling studies that produced EECO temperatures at 4480 ppmv $CO_2$ equivalent (Huber and Caballero, 2011 (Figure 17 ). Temperatures are similar when using the $TEX_{86}^{L}$ calibration for SST records (red numbers in Figure 17). However, $TEX_{86}^{H}$ seems to perform better, i.e. it shows higher coefficients in its relationship with the global core top dataset, than $TEX_{86}^{L}$, especially at high temperatures (Kim et al., 2010). When $TEX_{86}^{H}$ SST records are plotted at the AAG, ODP Site 1172 (Bijl et al., 2009) and Mid-Waipara river (Hollis et al., 2012), there is a ~5 °C mismatch between proxies and data (yellow numbers in Figure 17), revealing the problems in the model-proxy mismatch. Comparison of EECO records with equatorial records is complicated, as there is a lack of data in these regions. Sparse data from the equator shows a less than 2 °C difference between the equator and the southwest Pacific (Inglis et al., 2015), suggesting a southern hemisphere low meridional temperature gradient. High terrestrial temperatures (~23-26 °C) are recorded in the northern hemisphere mid latitudes (Inglis et al., 2017), while thermophilic paleovegetation is observed in the northern high latitudes (Akhmetiev, 2010). Moreover, high SSTs (~26 °C) are recorded at the mid-high latitudes of the west Siberian Sea (Frieling et al., 2014). These records show that the EECO was a uniformly warm period, with high temperatures extending from the northern to southern high latitudes.

## 5 Conclusion

The Late Paleocene – Early Eocene marginal marine sediments of the Latrobe-1 core were studied for their GDGT-distribution, spore and pollen assemblages and dinocyst assemblages. The core comprises of the Pebble point formation (370-355 m), the Pember mudstone (~355-392 m) and the Dilwyn formation (~392- 96 m). The palynomorphs from the core indicate the sediments were deposited from 57.2 to ~51.5 Ma. At 67.35 m, the sediments have a Middle Eocene (~41-39 Ma) age, indicating that between 96.34 m and 67.35 m there is a ~10 Myr hiatus, known in the region as the mid-Lutetian gap. The PETM is chemostratigraphically recognized in the core by the carbon isotope excursion (CIE).

$TEX_{86}^{H}$ SST reconstruction on the core was problematic because of the low concentrations of the GDGTs and the high BIT-index and MI values. The relationship between the *i*GDGTs and *br*GDGTs suggest that a substantial amount of the *i*GDGTs are derived from land. Although the $TEX_{86}^{H}$ SST

record shows a lot of scatter, the general temperature evolution seems to be partially recorded as temperature increases are recorded during the PETM and EECO, similar to the $TEX_{86}^{H}$ record of ODP Site 1172 (Bijl et al., 2009).Appliance of a new derived calibration ('Frieling calibration') to limit the influence of the high BIT and MI values improves the SST record by removing scatter, and shows a less prominent warming during the PETM and EECO compared to the $TEX_{86}^{H}$ SST record.

Late Paleocene paleovegetation was characterized by rainforest gymnosperm taxa, with minor angiosperm elements, indicative of subtropical vegetation with high (year-round) precipitation. The proximity to the coastline with significant riverine input in the Paleocene is demonstrated by the high abundance of *Senegalinium* complex species, a low salinity tolerant dinocyst group.

At the onset of the PETM *Glaphyrocysta* peaks, a dinocyst associated with transgression, while the ratio of marine palynomorphs increase indicating a Late Paleocene transgression. Concomitant with the transgression, rainforest gymnosperm taxa get (partially) replaced by ferns and thermophilic angiosperms. The increasing presence of these pioneering species was probably due to a combination of warming and disturbance of the coastal ecosystem as a result of the transgression. Swamp-type vegetation and palms are present during the PETM-onset, while at peak-PETM conditions the first signs of mangrove vegetation (e.g. *Nypa*) and megathermal elements are recorded, reflecting the PETM warming (MAT > 24 °C). *Nypa* has been recognized in several sites in the region, attesting to its widespread occurrence during the PETM, and the low meridonial temperature gradient during the PETM. The tropical dinocyst genus *Apectodinium,* which has been recorded at many different sites in the world appears during the onset and reaches abundances of ~80% at peak-PETM. The PETM introduces several angiosperm lineages in the area, that can be recorded throughout the whole Early Eocene.

The Early Eocene Dilwyn formation starts with a decrease in SST after the PETM to pre-PETM values. This is reflected in the vegetation, as Late Paleocene rainforest gymnosperm taxa increase again, and angiosperms are only minor elements. Around ~54 Ma, angiosperms start to increase in relative abundance and diversity, possibly related to the ETM-2 and the overall rise in $CO_2$ towards the EECO.

The reappearance of megathermal elements (e.g. *Nypa*) occurs around ~53.4 Ma and could be seen as the beginning of the EECO. Temperature rise around that time is recorded throughout the whole region. A second peak of *Apectodinium* is recorded around ~53 Ma, and its timing suggests a link to the ETM-3. The presence of *Apectodinium* at several sites in the AAG and its absence at the ETP (Bijl, 2007) suggests regions under the influence of the Proto-Leeuwin current experienced higher SSTs than regions influenced by the Tasman current. Angiosperms are the dominant vegetation group in the EECO, while ferns and gymnosperms are only minor elements. Dominant angiosperms during the EECO (*Casuarinaceae*, *Proteaceae*) seem to be tolerant to low nutrient availability. The high abundance of dinocyst genus *Homotryblium*, which is recorded in the Latrobe-1 and several different sites in the region, suggests lagoonal conditions during the EECO.

The palynological record of the Latrobe-1 shows large similarities with records from adjacent basins in the AAG and records from New Zealand and the combination of these records reveal the low meridional temperature gradient during the PETM and EECO. The high temperatures recorded at the Northern margin of the AAG strongly support the near-tropical temperatures recorded at IODP Site U1356 at Wilkes land (Pross et al., 2012). The data from the Latrobe-1 shows that there is a mismatch between temperatures derived from climate model data and $TEX_{86}^{H}$ proxy data in the northern AAG. This mismatch shows similar temperature differences between proxy and model data that were previously produced for both the southern AAG and the southwest Pacific Ocean.

**Acknowledgements**

I would like to thank my supervisors Peter Bijl, Joost Frieling, Francien Peterse, Timme Donders and Appy Sluijs for their supervision, discussions and feedback. The people of the Marine Palynology and Paleoceanography and Organic Geochemistry group are thanked for their help with the project, either in the laboratory or elsewhere. Finally I would like to thank the students of room 5.17 and the fifth floor for creating a pleasurable environment to write my MSc thesis.

## References

Akhmetiev, M. A. (2010). Paleocene and Eocene floristic and climatic change in Russia and Northern Kazakhstan. Bull. Geosci, 85(1), 17-34.

Archer, V. (1977). Palynology of the Victorian Mines Department Latrobe 1 bore, Otway Basin. Unpublished Honours thesis, Monash University, Melbourne, Australia

Arditto, P. A. (1995). The eastern Otway Basin Wangerrip Group revisited using an integrated sequence stratigraphic methodology. APEA JOURNAL, 35, 372-372.

Augusto, L., Davies, T. J., Delzon, S., & Schrijver, A. (2014). The enigma of the rise of angiosperms: can we untie the knot?. Ecology letters, 17(10), 1326-1338.

Baker, G. (1950). Geology and physiography of the Moonlight Head district, Victoria. Proc. Roy. Soc. Vic, 60, 17-42.

Baker, G. (1953). The relationship of Cyclammina bearing sediments to the older Tertiary deposits southeast of Princetown, Victoria. Mem. Nat. Mus. Melb, 18, 125-134.

Barker, P. F., Diekmann, B., & Escutia, C. (2007). Onset of Cenozoic Antarctic glaciation. Deep Sea Research Part II: Topical Studies in Oceanography, 54(21), 2293-2307.

Bijl, P. K.: Late Paleocene to Early Eocene palaeo-environments in the Southwest Pacific (2007). MSc Thesis, Department of Biology, Utrecht University, Utrecht, 97 pp.

Bijl, P. K., Schouten, S., Sluijs, A., Reichart, G. J., Zachos, J. C., & Brinkhuis, H. (2009). Early Palaeogene temperature evolution of the southwest Pacific Ocean. Nature, 461(7265), 776-779.

Bijl, P.K., Sluijs, A. & Brinkhuis, H. (2013a). A magneto- and chemostratigraphically calibrated dinoflagellate cyst zonation of the early Palaeogene South Pacific Ocean. Earth-science Reviews, 124, (pp. 1-31)

Bijl, P.K., Pross, J., Warnaar, J., Stickley, C.E., Huber, M., Guerstein, R., Houben, A.J.P., Sluijs, A., Visscher, H., Brinkhuis, H. (2011). Environmental forcings of Paleogene Southern Ocean dinoflagellate biogeography. Paleoceanography 26, PA1202.

Bijl, P. K., Sluijs, A., & Brinkhuis, H. (2013a). A magneto-and chemostratigraphically calibrated dinoflagellate cyst zonation of the early Palaeogene South Pacific Ocean. Earth-Science Reviews, 124, 1-31.

Bijl, P.K., Bendle, J.A.P., Bohaty, S.M., Pross, J., Schouten, S., Tauxe, L., Stickley, C.E., McKay, R.M., Röhl, U., Olney, M., Sluijs, A., Escutia, C. & Brinkhuis, H. (2013b). Eocene cooling linked to early flow across the Tasmanian Gateway. Proceedings of the National Academy of Sciences of the United States of America, 110 (24), 9645-9650

Boreham, C. J., Blevin, J. E., Duddy, I., Newman, J., Liu, K., Middleton, H., Macphail, M. K & Cook, A. C. (2002). Exploring the potential for oil generation, migration and accumulation in Cape Sorell—1, Sorell Basin, offshore west Tasmania. APPEA J, 42, 405-435.

Bowen, G. J., B. J. Maibauer, M. J. Kraus, U. Rohl, T. Westerhold, A. Steimke, P. D. Gingerich, S. L. Wing, and W. C. Clyde (2015), Two massive, rapid releases of carbon during the onset of the Palaeocene-Eocene thermal maximum, Nat. Geosci., 8(1), 44–47.

Brinkhuis, H., & Schiøler, P. (1996). Palynology of the Geulhemmerberg Cretaceous/Tertiary boundary section (Limburg, SE Netherlands). Geologie en Mijnbouw, 75(2/3), 193-213.

Carpenter, R. J., Hill, R. S., Greenwood, D. R., Partridge, A. D., & Banks, M. A. (2004). No snow in the mountains: Early Eocene plant fossils from Hotham Heights, Victoria, Australia. Australian Journal of Botany, 52(6), 685-718.

Carpenter, R. J., Jordan, G. J., Macphail, M. K., & Hill, R. S. (2012). Near-tropical Early Eocene terrestrial temperatures at the Australo-Antarctic margin, western Tasmania. Geology, 40(3), 267-270.

Close, D. I., Watts, A. B., & Stagg, H. M. J. (2009). A marine geophysical study of the Wilkes Land rifted continental margin, Antarctica. Geophysical Journal International, 177(2), 430-450.

Contreras, L., Pross, J., Bijl, P.K., Koutsodendris, A., Raine, J.I., van de Schootbrugge, B. & Brinkhuis, H. (2013). Early to Middle Eocene vegetation dynamics at the Wilkes Land Margin (Antarctica). Review of Palaeobotany and Palynology, 197, 119-142

Contreras, L., Pross, J., Bijl, P.K., O'Hara, R.B., Raine, J.I., Sluijs, A. & Brinkhuis, H. (2014). Southern high-latitude terrestrial climate change during the Palaeocene-Eocene derived from a marine pollen record (ODP Site 1172, East Tasman Plateau). Climate of the Past, 10 (4),1401-1420

Cookson, I. (1950). Fossil pollen grains of proteaceous type from Tertiary deposits in Australia. Australian Journal of Biological Sciences, 3(2), 166-177.

Cookson, I. C., & Pike, K. M. (1954). Some dicotyledonous pollen types from Cainozoic deposits in the Australian region. Australian journal of botany, 2(2), 197-219.

Cookson, I. C., & Eisenack, A. (1965). Microplankton from the Paleocene Pebble Point Formation, south-western Victoria. Proceedings of the Royal Society of Victoria, 79, 139-146.

Dawson, J. O. (2007). Ecology of actinorhizal plants. In Nitrogen-fixing actinorhizal symbioses (pp. 199-234). Springer Netherlands.

Dettman, M. E. (1965). Palynology of core samples from Yangery No.1, Laang No.1, Belfast No.4, Heywood No.10, Narrawaturk No.2, Portland No.3, Latrobe No.1 and Ecklin no.3 bores. Unpublished report submitted to Frome-Broken Hill Co. Pty. Ltd. 31/5/65

De Jonge, C., Hopmans, E. C., Zell, C. I., Kim, J. H., Schouten, S., & Damsté, J. S. S. (2014). Occurrence and abundance of 6-methyl branched glycerol dialkyl glycerol tetraethers in soils: Implications for palaeoclimate reconstruction. Geochimica et Cosmochimica Acta, 141, 97-112.

Dirghangi, S. S., Pagani, M., Hren, M. T., & Tipple, B. J. (2013). Distribution of glycerol dialkyl glycerol tetraethers in soils from two environmental transects in the USA. Organic Geochemistry, 59, 49-60.

Douglas, P. M., Affek, H. P., Ivany, L. C., Houben, A. J., Sijp, W. P., Sluijs, A., Schouten, S. & Pagani, M. (2014). Pronounced zonal heterogeneity in Eocene southern high-latitude sea surface temperatures. Proceedings of the National Academy of Sciences, 111(18), 6582-6587.

Edwards, J., Leonard, J. G., Pettifer, G. R., & McDonald, P. A. (1996). Colac 1: 250 000 geological map sheet—explanatory notes. Geological Survey of Victoria, Melbourne.

Eglington, C. (2006). Palaeogene Ostracoda (Crustacea) from the Wangerrip Group, Latrobe-1 bore, Otway Basin, Victoria, Australia. PROCEEDINGS-ROYAL SOCIETY OF VICTORIA, 118(1), 87.

Eglington, C. (2014) Sydney, Australia : Macquarie University. Taxonomy, evolution, biogeography and palaeoenvironmental significance of Victorian Paleogene ostracoda. PhD Thesis.

Fensome, R.A. and Williams, G.L., 2004. The Lentin and Williams Index of fossil dinoflagellates 2004 Edition. American Association of Stratigraphic Palynologists, Contributions Series, no. 42, 909p.

Foster, C. B. (1982). Illustrations of early Tertiary (Eocene) plant microfossils from the Yaamba Basin, Queensland (No. 381). Queensland Department of Mines.

Frieling, J., Iakovleva, A. I., Reichart, G. J., Aleksandrova, G. N., Gnibidenko, Z. N., Schouten, S., & Sluijs, A. (2014). Paleocene–Eocene warming and biotic response in the epicontinental West Siberian Sea. Geology, 42(9), 767-770.

Frieling, J. (2016). Climate, carbon cycling and marine ecology during the Paleocene-Eocene Thermal Maximum (Doctoral dissertation, UU Dept. of Earth Sciences).

Frieling, J., Gebhardt, H., Huber, M., Adekeye, O. A., Akande, S. O., Reichart, G. J., Middelburg, J. J., Schouten, S. & Sluijs, A. (2017). Extreme warmth and heat-stressed plankton in the tropics during the Paleocene-Eocene Thermal Maximum. Science advances, 3(3), e1600891.

Geological Survey of Victoria (1995). The stratigraphy, structure, geophysics and hydrocarbon potential of the Eastern Otway Basin. Geological Survey of Victoria Report 103.

Gradstein, F. M., Ogg, J. G., Smith, A. G., Bleeker, W., & Lourens, L. J. (2004). A new geologic time scale, with special reference to Precambrian and Neogene. Episodes, 27(2), 83-100.

Gradstein, F. M., Ogg, J. G., Schmitz, M., & Ogg, G. (Eds.). (2012). The geologic time scale 2012. elsevier.

Greenwood, D. R., Moss, P. T., Rowett, A. I., Vadala, A. J., & Keefe, R. L. (2003). Plant communities and climate change in southeastern Australia during the early Paleogene. SPECIAL PAPERS-GEOLOGICAL SOCIETY OF AMERICA, 365-380.

Handley, L., Crouch, E. M., & Pancost, R. D. (2011). A New Zealand record of sea level rise and environmental change during the Paleocene–Eocene Thermal Maximum. Palaeogeography, Palaeoclimatology, Palaeoecology, 305(1), 185-200.

Harris, W. K. (1965). Basal tertiary microfloras from the Princetown area, Victoria, Australia. Palaeontographica Abteilung B, 75-106.

Hines, B. R., Hollis, C. J., Atkins, C. B., Baker, J. A., Morgans, H. E., & Strong, P. C. (2017). Reduction of oceanic temperature gradients in the early Eocene Southwest Pacific Ocean. Palaeogeography, Palaeoclimatology, Palaeoecology, 475, 41-54.

Ho, S. L., & Laepple, T. (2016). Flat meridional temperature gradient in the early Eocene in the subsurface rather than surface ocean. Nature Geoscience, 9(8), 606-610.

Holdgate, G. R., & Clarke, J. D. (2000). A Review of Tertiary Brown Coal Deposits in Australia--Their Depositional Factors and Eustatic Correlations. AAPG bulletin, 84(8), 1129-1151.

Holdgate, G. R., Smith, T. A. G., Gallagher, S. J., & Wallace, M. W. (2001). Geology of coal-bearing Palaeogene sediments, onshore Torquay Basin, Victoria. Australian Journal of Earth Sciences, 48(5), 657-679.

Holdgate, G. & Gallagher, S. J., (2003). In: Birch W. D. (Editor) 2003. Geology of Victoria. Geological Society of Australia Special Publication 23. Geological Society of Australia (Victoria Division)

Holford, S. P., Tuitt, A. K., Hillis, R. R., Green, P. F., Stoker, M. S., Duddy, I. R., Sandiford, M. & Tassone, D. R. (2014). Cenozoic deformation in the Otway Basin, southern Australian margin: implications for the origin and nature of post-breakup compression at rifted margins. Basin Research, 26(1), 10-37.

Hollis, C.J., Handley, L., Crouch, E.M., Morgans, H.E.G., Baker, J.A., Creech, J., Collins, K.S., Gibbs, S.J., Huber, M., Schouten, S., Zachos, J.C., Pancost, R.D. (2009). Tropical sea temperatures in the high-latitude South Pacific during the Eocene. Geology 37, 99–102.

Hollis, C. J., Taylor, K. W., Handley, L., Pancost, R. D., Huber, M., Creech, J. B., B. R., Hines, E. M., Crouch, H. E. G., Morgans, J. S., Crampton, S. Gibbs, P. N., Pearson & Zachos, J. C. (2012). Early Paleogene temperature history of the Southwest Pacific Ocean: Reconciling proxies and models. Earth and planetary science letters, 349, 53-66.

Hopmans, E. C., Weijers, J. W., Schefuß, E., Herfort, L., Damsté, J. S. S., & Schouten, S. (2004). A novel proxy for terrestrial organic matter in sediments based on branched and isoprenoid tetraether lipids. Earth and Planetary Science Letters, 224(1), 107-116.

Hopmans, E. C., Schouten, S., & Damsté, J. S. S. (2016). The effect of improved chromatography on GDGT-based palaeoproxies. Organic Geochemistry, 93, 1-6.

Huber, M., Brinkhuis, H., Stickley, C. E., Döös, K., Sluijs, A., Warnaar, J., S.A., Schellenberg & Williams, G. L. (2004). Eocene circulation of the Southern Ocean: Was Antarctica kept warm by subtropical waters?. Paleoceanography, 19(4).

Huber, M., & Caballero, R. (2011). The early Eocene equable climate problem revisited. Climate of the Past, 7(2), 603-633.

Inglis, G. N., Farnsworth, A., Lunt, D., Foster, G. L., Hollis, C. J., Pagani, M., Jardine, P.E., Pearson, P.N., Markwick, P., Galsworthy, A.M. & Raynham, L. (2015). Descent toward the Icehouse: Eocene sea surface cooling inferred from GDGT distributions. Paleoceanography, 30(7), 1000-1020.

Inglis, G. N., Collinson, M. E., Riegel, W., Wilde, V., Farnsworth, A., Lunt, D. J., Valdes, P. Robson, B.E., Scott, A.C., Lenz, O.K., Naafs, B. D. A. & Pancost, R.D. (2017). Mid-latitude continental temperatures through the early Eocene in western Europe. Earth and Planetary Science Letters, 460, 86-96.

Jagniecki, E. A., Lowenstein, T. K., Jenkins, D. M., & Demicco, R. V. (2015). Eocene atmospheric CO2 from the nahcolite proxy. Geology, 43(12), 1075-1078.

Jones, T. D., Lunt, D. J., Schmidt, D. N., Ridgwell, A., Sluijs, A., Valdes, P. J., & Maslin, M. (2013). Climate model and proxy data constraints on ocean warming across the Paleocene–Eocene Thermal Maximum. Earth-Science Reviews, 125, 123-145.

Kim, J. H., Van der Meer, J., Schouten, S., Helmke, P., Willmott, V., Sangiorgi, F F., Koç, N., Hopmans, E.C.,& Damsté, J. S. S. (2010). New indices and calibrations derived from the distribution of crenarchaeal isoprenoid tetraether lipids: Implications for past sea surface temperature reconstructions. Geochimica et Cosmochimica Acta, 74(16), 4639-4654.

Karthikeyan, A. (2016). Impact of elevated CO2 in Casuarina equisetifolia rooted stem cuttings inoculated with Frankia. Symbiosis, 1-6.

Krassay, A. A., Cathro, D. L., & Ryan, D. J. (2004). A regional tectonostratigraphic framework for the Otway Basin. In Eastern Australasian Basins Symposium II, Petroleum Exploration Society of Australia, Special Publication (pp. 97-116).

Lauretano, V., Hilgen, F. J., Zachos, J. C., & Lourens, L. J. (2016). Astronomically tuned age model for the early Eocene carbon isotope events: A new high-resolution δ13 Cbenthic record of ODP Site 1263 between~ 49 and~ 54 Ma. Newsletters on Stratigraphy, 49(2), 383-400.

Louwye, S., & Laga, P. (2008). Dinoflagellate cyst stratigraphy and palaeoenvironment of the marginal marine Middle and Upper Miocene of the eastern Campine area, northern Belgium (southern North Sea Basin). Geological Journal, 43(1), 75-94.

Macphail, M. K., Alley, N. F., Truswell, E. M., & Sluiter, I. R. K. (1994). Early Tertiary vegetation: evidence from spores and pollen. In 'History of the Australian vegetation: Cretaceous to recent'.(Ed. RS Hill) pp. 189–261.

Macphail, M. K. (1999). Palynostratigraphy of the Murray Basin, inland southeastern Australia. Palynology, 23(1), 197-240.

Macphail M. (2007). Australian Palaeoclimates: Cretaceous to Tertiary - A review of palaeobotanical and related evidence to the year 2000. CRC LEME Special Volume Open File Report 151, 266pp.

Macphail, M. K. (2013). Preliminary palynostratigraphic age determinations on core from Strahan BH-1, Macquarie Harbour, western Tasmania.

McGowran, B., Holdgate, G. R., Li, Q., & Gallagher, S. J. (2004). Cenozoic stratigraphic succession in southeastern Australia. Australian Journal of Earth Sciences, 51(4), 459-496.

McInerney, F. A., & Wing, S. L. (2011). The Paleocene-Eocene Thermal Maximum: A perturbation of carbon cycle, climate, and biosphere with implications for the future. Annual Review of Earth and Planetary Sciences, 39, 489-516.

Megallaa, M. (1986). Tectonic development of Victoria's Otway Basin—a seismic interpretation. In Second South-Eastern Australian Oil Exploration Symposium, Petroleum Exploration Society of Australia (pp. 201-218).

Milne, L.A., 1988. Palynology of a late Eocene lignitic sequence from the western margin of the Eucla Basin, Western Australia. Assoc. Australas. Palaeontol. Mem., 5: 285-310.

Ngom, M., Gray, K., Diagne, N., Oshone, R., Fardoux, J., Gherbi, H., Hocher, V., Svistoonoff, S., Laplaze, L., Tisa, L.S., Sy, M. O., & Champion, A. (2016). Symbiotic performance of diverse Frankia strains on salt-stressed Casuarina glauca and Casuarina equisetifolia plants. Frontiers in Plant Science, 7.

Ngom M, Gray K, Diagne N, Oshone R, Fardoux J, Gherbi H, , Sy MO and (2016) Symbiotic Performance of Diverse Frankia Strains on Salt-Stressed Casuarina glauca and Casuarina equisetifolia Plants. Front. Plant Sci. 7:1331

Pancost, R.D., Taylor, K.W.R., Inglis, G.N., Kennedy, E.M., Handley, L., Hollis, C.J., Crouch, E. M., Pross, J., Huber, M., Schouten, S., Pearson, P.N., Morgans, H.E.G., Raine, J.I. (2013). Early Paleogene evolution of terrestrial climate in the SW Pacific, Southern New Zealand. Geochem. Geophys. Geosyst.

Partridge, A.D., (1999). Late Cretaceous to Tertiary geological evolution of the Gippsland Basin [Ph.D. thesis]: Bundoora, Australia, Latrobe University, 439 p.

Partridge, A. (2002). Bass Basin palynological project. Unravelling a Late Cretaceous to Eocene geological history of large palaeolakes, coastal lagoons and marine bays. Appendix C8 in: Blevin, J. 2003.

Partridge, A.D., (2006) Late Cretaceous–Cenozoic palynology zonations Gippsland Basin [chart], in Monteil, E., coordinator, Australian Mesozoic and Cenozoic palynology zonations— Updated to the 2004 geologic time scale: Geoscience Australia Record 2006/23.

Pearson, P. N., van Dongen, B. E., Nicholas, C. J., Pancost, R. D., Schouten, S., Singano, J. M., & Wade, B. S. (2007). Stable warm tropical climate through the Eocene Epoch. Geology, 35(3), 211-214.

Peterse F., van der Meer J., Schouten S., Weijers J. W. H., Fierer N., Jackson R. B., Kim J.-H. and Sinninghe Damste´ J. S. (2012). Revised calibration of the MBT–CBT paleotemperature proxy based on branched tetraether membrane lipids in surface soils. Geochim. Cosmochim. Acta 96, 215–229.

Pocknall, D. T., & Crosbie, Y. M. (1982). Taxonomic revision of some Tertiary tricolporate and tricolpate pollen grains from New Zealand. New Zealand journal of botany, 20(1), 7-15.

Pocknall, D. T. (1990). Palynological evidence for the early to middle Eocene vegetation and climate history of New Zealand. Review of palaeobotany and palynology, 65(1-4), 57-69.

Pole, M. (2010). Ecology of Paleocene-Eocene vegetation at Kakahu, South Canterbury, New Zealand. Palaeontologia Electronica, 13, 29.

Pross, J., Contreras, L., Bijl, P.K., Greenwood, D.R., Bohaty, S.M., Schouten, S., Bendle, J.A., Röhl, U., Tauxe, L., Raine, J.I., Huck, C.E., van de Flierdt, T., Jamieson, S.S.R., Stickley, C.E., van de Schootbrugge, B., Escutia, C. & Brinkhuis, H. (2012). Persistent near-tropical warmth on the Antarctic continent during the early Eocene epoch. Nature, 488, 73-77

Raine, J.I., Mildenhall, D.C., Kennedy E.M. (2011). New Zealand fossil spores and pollen: an illustrated catalogue. 4th edition. GNS Science miscellaneous series no. 4.

Reichart, G. J., Brinkhuis, H., Huiskamp, F., & Zachariasse, W. J. (2004). Hyperstratification following glacial overturning events in the northern Arabian Sea. Paleoceanography, 19(2).

Schiøler, P., Brinkhuis, H., Roncaglia, L., & Wilson, G. J. (1997). Dinoflagellate biostratigraphy and sequence stratigraphy of the type Maastrichtian (Upper Cretaceous), ENCI Quarry, The Netherlands. Marine Micropaleontology, 31(1), 65-95.

Schouten, S., Hopmans, E. C., Schefuß, E., & Damste, J. S. S. (2002). Distributional variations in marine crenarchaeotal membrane lipids: a new tool for reconstructing ancient sea water temperatures?. Earth and Planetary Science Letters, 204(1), 265-274.

Schouten, S., Hopmans, E. C., & Damsté, J. S. S. (2013). The organic geochemistry of glycerol dialkyl glycerol tetraether lipids: a review. Organic geochemistry, 54, 19-61.

Self-Trail, J. M., Powars, D. S., Watkins, D. K., & Wandless, G. A. (2012). Calcareous nannofossil assemblage changes across the Paleocene–Eocene Thermal Maximum: Evidence from a shelf setting. Marine Micropaleontology, 92, 61-80.

Shepherd, C. L. (2017). Early to middle Eocene calcareous nannofossils of the SW Pacific: Paleobiogeography and paleoclimate. PhD Thesis.

Sigurdsson, B. D., Medhurst, J. L., Wallin, G., Eggertsson, O., & Linder, S. (2013). Growth of mature boreal Norway spruce was not affected by elevated [CO2] and/or air temperature unless nutrient availability was improved. Tree physiology, 33(11), 1192-1205.

Slotnick, B. S., Dickens, G. R., Nicolo, M. J., Hollis, C. J., Crampton, J. S., Zachos, J. C., & Sluijs, A. (2012). Large-amplitude variations in carbon cycling and terrestrial weathering during the latest Paleocene and earliest Eocene: The record at Mead Stream, New Zealand. The journal of geology, 120(5), 487-505.

Slotnick, B. S., Dickens, G. R., Hollis, C. J., Crampton, J. S., Percy Strong, C., & Phillips, A. (2015). The onset of the early Eocene climatic optimum at branch stream, Clarence River valley, New Zealand. New Zealand Journal of Geology and Geophysics, 58(3), 262-280.

Sluijs, A., Pross, J., & Brinkhuis, H. (2005). From greenhouse to icehouse; organic-walled dinoflagellate cysts as paleoenvironmental indicators in the Paleogene. Earth-Science Reviews, 68(3), 281-315.

Sluijs, A., Schouten, S., Pagani, M., Woltering, M., Brinkhuis, H., Sinninghe Damste´, J.S., Dickens, G.R., Huber, M., Reichart, G.-J., Stein, R., Matthiessen, J., Lourens, L.J., Pedentchouk, N., Backman, J., Moran, K. & the Expedition 302 Scientists (2006). Subtropical Arctic Ocean temperatures during the Palaeocene-Eocene thermal maximum. Nature 441, 610–613.

Sluijs, A., Brinkhuis, H., Schouten, S., Zachos, J.C., Bohaty, S., John, C., Deltrap, R., Reichart, G.J., Sinninghe Damsté, J.S., Crouch, E., Dickens, G.R., (2007). Environmental precursors to rapid light carbon injection at the Palaeocene/ Eocene boundary. Nature 450, 1218–1221.

Sluijs, A., Röhl, U., Schouten, S., Brumsack, H. J., Sangiorgi, F., Sinninghe Damsté, J. S., & Brinkhuis, H. (2008a). Arctic late Paleocene–early Eocene paleoenvironments with special emphasis on the Paleocene-Eocene thermal maximum (Lomonosov Ridge, Integrated Ocean Drilling Program Expedition 302). Paleoceanography, 23(1).

Sluijs, A., Brinkhuis, H., Crouch, E. M., John, C. M., Handley, L., Munsterman, D., Bohaty, S.M., Zachos, J.C., Reichart, G.-J., Schouten, S., Pancost, R.D., Sinninghe Damsté, J.S., Welters, N.L.D., Lotter, A.F., Dickens, G.R. (2008b). Eustatic variations during the Paleocene-Eocene greenhouse world. Paleoceanography, 23(4).

Sluijs, A., Brinkhuis, H., Williams, G. L., & Fensome, R. A. (2009a). Taxonomic revision of some Cretaceous–Cenozoic spiny organic-walled peridiniacean dinoflagellate cysts. Review of Palaeobotany and Palynology, 154(1), 34-53.

Sluijs, A., & Brinkhuis, H. (2009b). A dynamic climate and ecosystem state during the Paleocene-Eocene Thermal Maximum: Inferences from dinoflagellate cyst assemblages on the New Jersey Shelf. Biogeosciences, 6(8), 1755-1781.

Sluijs, A., Bijl, P. K., Schouten, S., Röhl, U., Reichart, G. J., & Brinkhuis, H. (2011). Southern ocean warming, sea level and hydrological change during the Paleocene-Eocene thermal maximum. Climate of the Past, 7(1), 47-61.

Stilwell, J. D. (2003). Macropalaeontology of the Trochocyathus-Trematotrochus band (Paleocene/Eocene boundary), Dilwyn Formation, Otway Basin, Victoria. Alcheringa, 27(4), 245-275.

Stover, L. E., & Partridge, A. D. (1973). Tertiary and Late Cretaceous spores and pollen from the Gippsland Basin, southeastern Australia. Proceedings of the Royal Society of Victoria, 85(2), 237-286.

Suan, G., Popescu, S. M., Suc, J. P., Schnyder, J., Fauquette, S., Baudin, F., Yoon, D., Piepjohn, K., Sobolev, N. N. & Labrousse, L. (2017). Subtropical climate conditions and mangrove growth in Arctic Siberia during the early Eocene. Geology, 45(6), 539-542.

Taylor, D. J., (1964). Biostratigraphic log Latrobe No. 1 bore. Geological Survey of Victoria, Unpublished Report, PE990957, Department of Manufacturing and Industry Development, Melbourne, 1-3.

Taylor, D. J., (1965). Preservation, composition, and significance of Victorian Lower Tertiary 'Cyclammina faunas'. Proceedings of the Royal Society of Victoria, N. S. 78(2), 143-160.

Thomas, D. J., Bralower, T. J., & Jones, C. E. (2003). Neodymium isotopic reconstruction of late Paleocene–early Eocene thermohaline circulation. Earth and Planetary Science Letters, 209(3), 309-322.

Tickell, S.J. , Edwards, J. , Abele, C. 1992 Port Campbell Embayment 1:100 000 map, geological report. Geological Survey of Victoria. Report 95

Turner, S. K., & Ridgwell, A. (2016). Development of a novel empirical framework for interpreting geological carbon isotope excursions, with implications for the rate of carbon injection across the PETM. Earth and Planetary Science Letters, 435, 1-13.

Wall, D., Dale, B., Lohmann, G. P., & Smith, W. K. (1977). The environmental and climatic distribution of dinoflagellate cysts in modern marine sediments from regions in the North and South Atlantic Oceans and adjacent seas. Marine micropaleontology, 2, 121-200.

Ward, P. D., Flannery, D., Flannery, E., & Flannery, T. F. (2016). The Paleocene cephalopod fauna from pebble point, Victoria (Australia)-fulcrum between two Eras. Memoirs of Museum Victoria, 74 391-402.

Wilson, G. J. (1988). Paleocene and Eocene dinoflagellate cysts from Waipawa, Hawkes Bay, New Zealand (No. 57). New Zealand Geological Survey.

Wing, S. L., & Currano, E. D. (2013). Plant response to a global greenhouse event 56 million years ago. American journal of botany, 100(7), 1234-1254.

Yu, S. M. (1988). Structure and development of the Otway Basin. The APEA Journal, 28(1), 243-253.

Zachos, J. C., Dickens, G. R., & Zeebe, R. E. (2008). An early Cenozoic perspective on greenhouse warming and carbon-cycle dynamics. Nature, 451(7176), 279-283.

Zeebe, R. E., Ridgwell, A., & Zachos, J. C. (2016). Anthropogenic carbon release rate unprecedented during the past 66 million years. Nature Geoscience, 9(4), 325-329.

Zhang, Y. G., Pagani, M., & Wang, Z. (2016). Ring Index: A new strategy to evaluate the integrity of TEX86 paleothermometry. Paleoceanography. 31, 220–232.

# Appendix

**Contents**



1. Plate 1 – Scale bar = 25 µm

a) Apectodinium homomorphum
b) Apectodinium hyperacanthum
c) Apectodinium quinqelatum
d) Homotryblium tasmaniense
e) Cleistosphaeridium polypetellum
f) Diphyes colligerum
g) Systemataphora variabilis
h) Cerodinium obliquipes/pachyceros
i) Phtanoperidinium sp.
j) Phtanoperidinium sp.
k) Senegalinium sp.
l) Senegalinium dilwynense
m) Spinidinium sp.
n) Spinidinium sp.
o) Vozzhennikovia roehlia

2. Plate 2 – Scale bar = 25 µm

a) Rhombodinium subtile
b) Rhombodinium subtile
c) Paralecaniella
d) Dilwynites granulatus
e) Gleicheniidites senonicus
f) Haloragicidites harrisii
g) Malvacipollis subtilis
h) Matonisporites gigantis
i) Myrtaceidites tenuis
j) Podocarpidites ellipticus
k) Proteacidites tuberculiformis
l) Proteacidites pachypolis
m) Spinizonocolpites prominatus

Plate 1

a

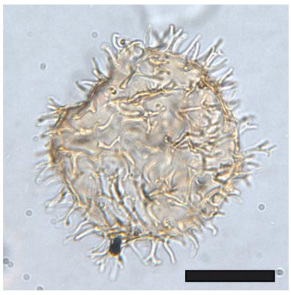

b

c

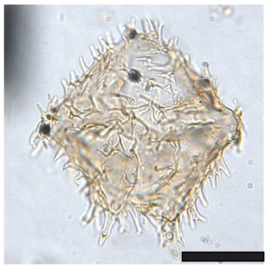

d

e

f

g

h

i

j

k

l

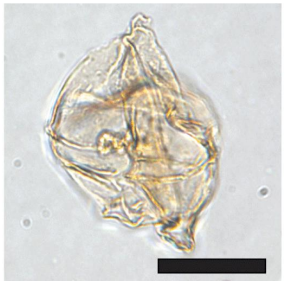

m

n

o

Plate 2

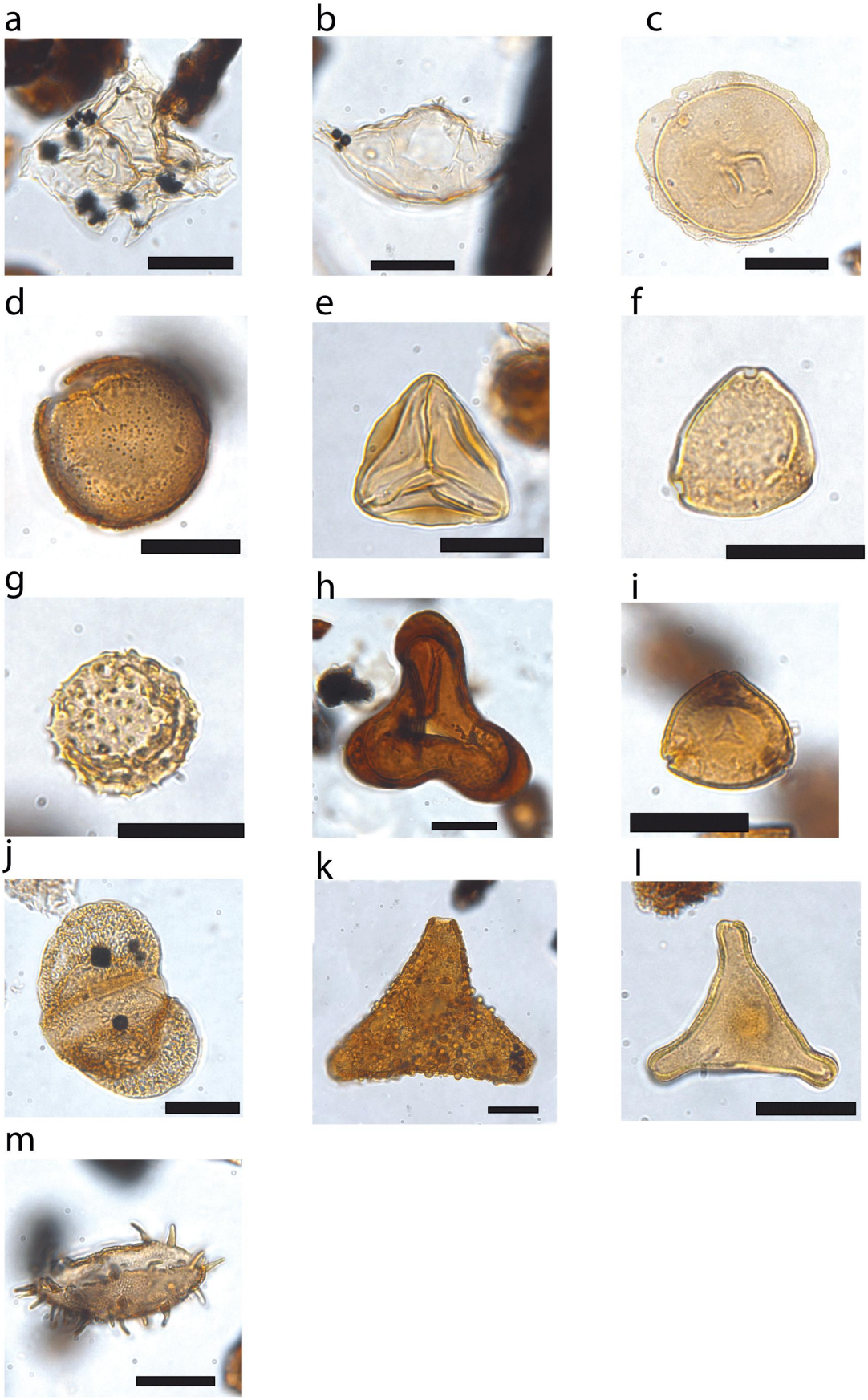

3.

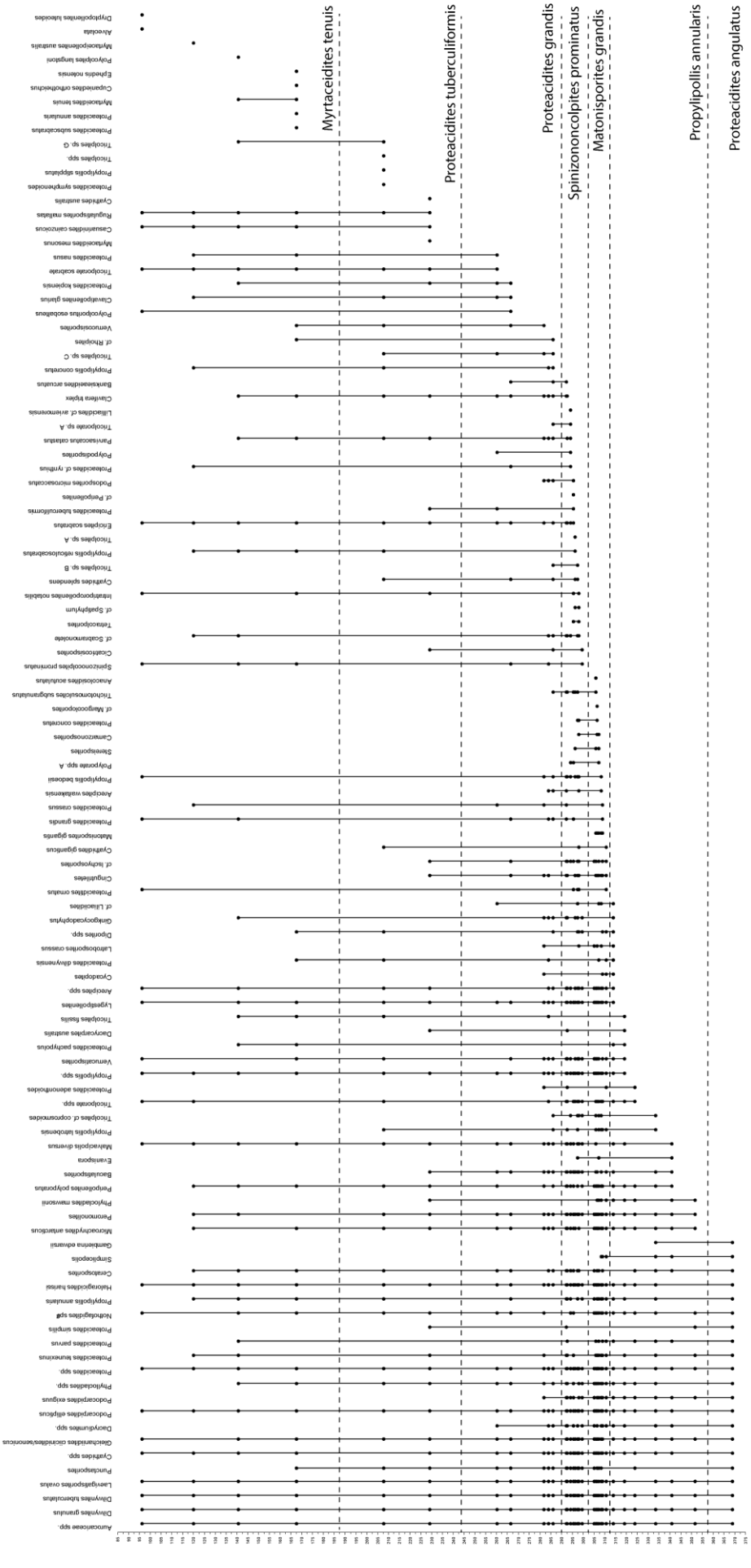


**Figure 2. Range chart for the spores and pollen encountered in the Latrobe-1 core**

4.

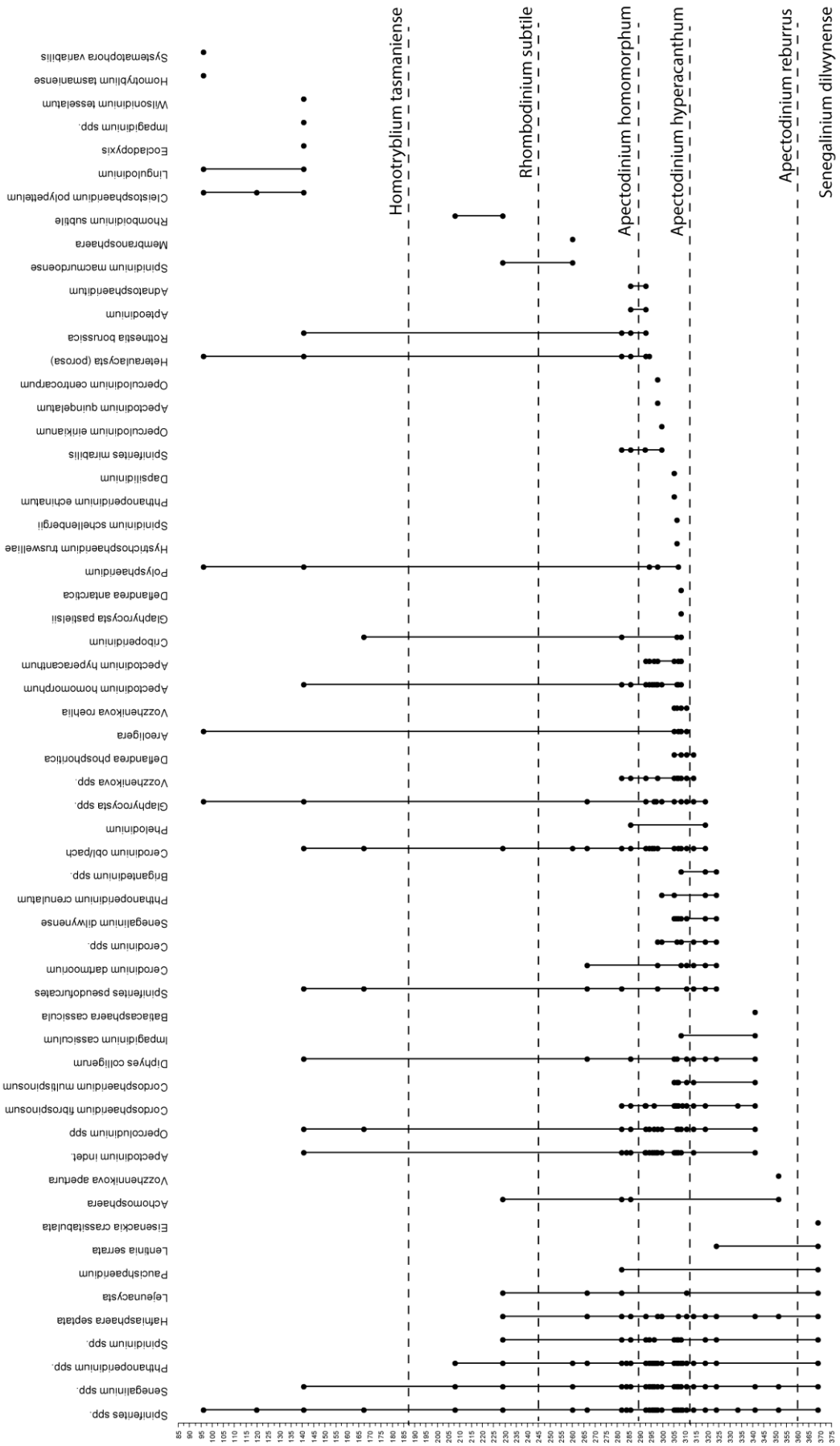


**Figure 2. Range chart for the dinocysts encountered in the Latrobe-1 core**

5.

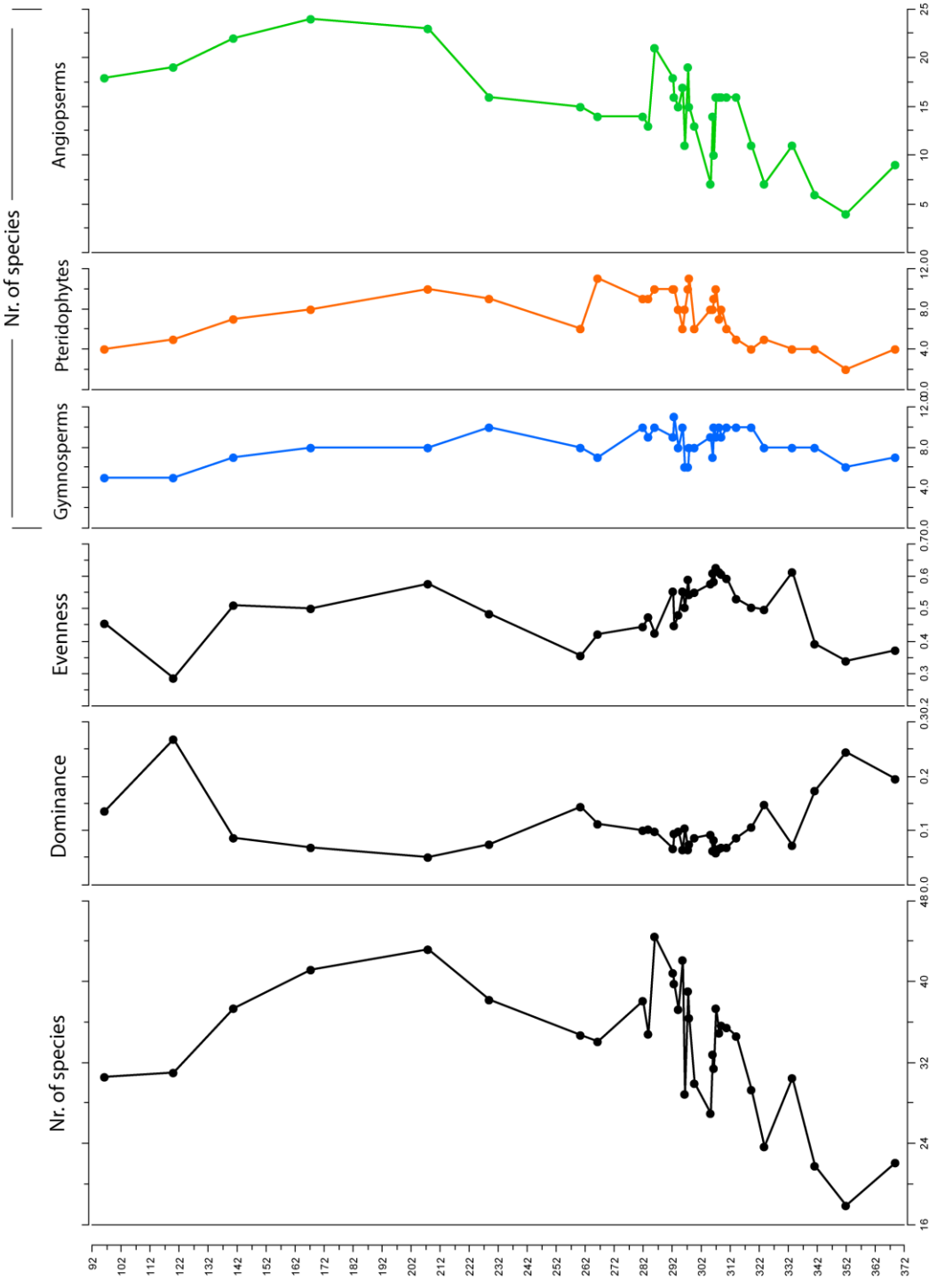


***Figure 3.*** *Nr of species (rarefied at 200 specimens), Dominance, Evenness and nr. Of species for the specific plant types*